The Radiation Environment for the Next Generation Space Telescope

<Document Control Number>

Janet L. Barth

NASA/Goddard Space Flight Center
Greenbelt, Maryland

John C. Isaacs

Space Telescope Science Institute
Baltimore, Maryland

December 1999

Table of Contents

I. Introduction

The purpose of this document is to define the radiation environment for the evaluation of degradation due to total ionizing and non-ionizing dose and of single event effects (SEEs) for the Next Generation Space Telescope (NGST) instruments and spacecraft. The analysis took into account the radiation exposure for the nominal five-year mission at the Earth-Sun L2 Point and assumes a launch date of 2008. The transfer trajectory out to the L2 position has not yet been defined, therefore, this evaluation does not include the impact of passing through the Van Allen belts. Generally, transfer trajectories do not contribute to degradation effects; however, single event effects must be taken into consideration especially if critical maneuvers are planned during the Van Allen belt passes.

II. Radiation Environment

The natural space radiation environment of concern for damage to spacecraft electronics is classified into two populations, 1) the transient particles which include protons and heavier ions of all of the elements of the periodic table, and 2) the trapped particles which include protons, electrons and heavier ions. The trapped electrons have energies up to 10 MeV and the trapped protons and heavier ions have energies up to 100s of MeV. The transient radiation consists of galactic cosmic ray particles and particles from solar events (coronal mass ejections and flares). The cosmic rays have low level fluxes with energies up to TeV. The solar eruptions periodically produce energetic protons, alpha particles, heavy ions, and electrons. The solar protons have energies up to 100's MeV and the heavier ions reach the GeV range. All particles are isotropic and omnidirectional.

Space also contains low energy plasma of electrons and protons with fluxes up to 10^{12} cm^2/sec. The plasmasphere environment and the low energy (< 0.1 MeV) component of the charged particles are a concern in the near-earth environment. In the outer regions of the magnetosphere and in interplanetary space, the plasma is associated with the solar wind. Because of its low energy, thin layers of material easily stop the plasma so it is not a hazard to most spacecraft electronics. However, it is damaging to surface materials and differentials in the plasma environment can contribute to spacecraft surface charging and discharging problems [1,2].

III. Description of Radiation Effects

Radiation effects that are important to consider for instrument and spacecraft design fall roughly into three categories: degradation from total ionizing dose (TID), degradation from non-ionizing energy loss (NIEL), and single event effects. Total ionizing dose in electronics is a cumulative long term ionizing damage due to protons and electrons. It causes threshold shifts, leakage current and timing skews. The effect first appears as parametric degradation of the device and ultimately results in functional failure. It is possible to reduce TID with shielding material that absorbs most electrons and lower energy protons. As shielding is increased, shielding effectiveness decreases because of the difficulty in slowing down the higher energy protons. When a manufacturer advertises a part as "rad-hard", he is almost always referring to its total ionizing dose characteristics. Rad-hard does not usually imply that the part is hard to non-ionizing dose or single event effects.

Displacement damage is cumulative long-term non-ionizing damage due to protons, electrons, and neutrons. The particles produce defects in optical materials that result in charge transfer degradation. It affects the performance of optocouplers (often a component in power devices), solar cells, CCDs, and linear bipolar devices. The effectiveness of shielding depends on the location of the device. For example, coverglasses over solar cells reduce electron damage and proton damage by absorbing the low energy particles. Increasing shielding, however, is not usually effective for optoelectronic components because the high-energy protons penetrate the most feasible spacecraft electronic enclosures.

Single event effects are caused through ionization by a single charged particle as it passes through a sensitive junction of an electronic device. They are caused by heavier ions, but for some devices, protons can induce single event effects. In some cases SEEs are induced through direct ionization by the proton, but in most instances, proton induced effects are the result of secondary particles that are produced when the proton collides with a nucleus of the material in the device. Some single event effects are non-destructive as in the case of single event upsets (SEUs), single event transients (SETs), multiple bit errors (MBEs), single event hard errors (SHEs), single event transients (SETs), etc. Single event effects can also be destructive as in the case of single event latchups (SELs), single event gate ruptures (SEGRs), and single event burnouts (SEBs). The severity of the effect can range from noisy data to loss of the mission. It is dependent on the type of effect and the criticality of the system in which it occurs. Shielding is not an effective mitigator for single event effects because they are induced by very penetrating high energy particles. The preferred method for dealing with destructive failures is to use SEE-hard parts. When SEE-hard parts are not available, latchup protection circuitry is sometimes used in conjunction with failure mode analysis. For non-destructive effects, mitigation takes the form of error-detection and correction codes (EDACs), filtering circuitry, etc.

Total ionizing dose is primarily caused by protons and electrons trapped in the Van Allen belts and solar event protons. As electrons are slowed down, their interactions with orbital electrons of the shielding material produce a secondary photon radiation known as bremsstrahlung. Generally, the dose due to galactic cosmic ray ions and proton secondaries is negligible in the presence of the other sources. For surface degradation, it is also important to include the effects of very low energy particles.

Single event effects can be induced by heavy ions (solar events and galactic cosmic rays) and, in some devices, protons (trapped and solar events) and neutrons. Displacement damage is primarily due to trapped and solar protons and also neutrons that are produced by interactions of primary particles with the atmosphere and spacecraft materials.[*]

IV. The NGST Mission

The NGST spacecraft will be transferred out to the L2 point via a trajectory that has not yet been defined. While in the transfer, NGST will pass through the trapped proton and electron belts. These exposures could constitute a single event effect risk during some maneuvers but will not contribute to significant degradation effects. During the transfer trajectory, NGST will also encounter varying levels of galactic cosmic ray heavy ions and possibly protons and heavier ions from solar events.

[*] In avionics applications it is necessary to consider neutrons that are produced by interactions of primary particles with the atmosphere.

Once NGST is at L2, its mission requirement is 5 years, and its mission goal is 10 years. With its expected 2008 launch date, the NGST mission will occur during both the inactive and active phases of the solar cycle. During the active phase of the sun, the likelihood that the spacecraft will be exposed to particles from solar events (either solar flare of coronal mass ejections) increases significantly. Based on an average 11-year solar cycle, the NGST mission will encounter 3 years of solar active conditions. The length of the solar cycle ranges from 9 to 13 years, so the 3-year estimate is not precise. Hence, this analysis also includes estimates for 2 and 4 years of solar active conditions. The active phase of the solar cycle occurs at the beginning of the mission (the first 2-4 years), therefore, extending the length of the mission from 5 up to 10 years does not have a significant impact on the degradation predictions for the NGST. The L2 radiation environment encountered by the NGST will consist of protons and heavier ions from solar events, galactic cosmic ray heavy ions, and solar wind plasma consisting of low energy protons, electrons, and heavier ions.

V. Total Dose and Degradation

The total ionizing dose accumulation causes performance degradation and failure on memories, power converters, etc. Non-ionizing energy loss in materials (atomic displacement damage) causes degradation of solar cells, optoelectronics, and detectors. The low energy particles also contribute to the erosion of surfaces.

A. Degradation Environment

At L2 low energy particles from the solar wind plasma contribute to the degradation of surface materials. The higher energy particles trapped in the Van Allen belts and from high energy solar events can penetrate solar cell coverglasses and solar array substrate structures and, therefore, are responsible for solar cell degradation.

1. The Plasma Environment

The solar wind is composed of protons and heavier ions (roughly 95% and H^+ and 5% H^{++}) combined with enough electrons to form an electrically neutral plasma. It is commonly described in terms of average density, velocity, and temperature. **Table 1** lists average values or a range of values for these parameters

Table 1
Average Solar Wind Parameters

Density	1-10 particles/cm^3
Velocity	400 km/s
Energy	“a few eV”

A model of the solar wind plasma that can be used for engineering applications such as material degradation analysis and spacecraft surface charging is not available at this time. However, a joint effort at GSFC and MFSC is underway to develop a plasma model for these applications. In the meantime, recent satellite measurements provide a good understanding of the dynamic range of the density, velocity, and energy temperature.

The plasma environment for the NGST spacecraft will depend on its position relative to the magnetotail region of the earth's magnetosphere.* The data given here from the GEOTAIL and SOHO spacecraft give a sampling of the expected range of the solar wind parameters inside and outside of the magnetotail. The SOHO spacecraft has also measured plasma parameters with the Mass Time-of-Flight/Proton Monitor. Measurements [3] are given here outside of the tail region at ~230 earth radii during January 1997. **Figures 1-3** plot the plasma density, velocity, and energy. A sampling of the data is given in **Table 2**. The data in the table and figures show that the average solar wind parameters given in Table 1 compare favorable with the SOHO measurements.

Table 2
SOHO CELIAS Proton Monitor Outside Magnetotail ~ 230-250 R_e

Substorm Conditions

Day	Hour	Density (#/cm^3)	Energy (eV)	Bulk Speed (km/s)
11	2	23.4	6.8	425
11	3	18.5	7.5	441
11	4	13.1	14.7	487
11	5	18.1	15.2	489
11	6	14.7	17.6	500

Relaxed Substorm Conditions (medium density/low bulk velocity)

Day	Hour	Density (#/cm^3)	Energy (eV)	Bulk Speed (km/s)
16	3	8.6	1.9	304
16	4	8.1	2.1	313
16	5	5.8	2.3	319
16	6	3.2	2.8	340
16	7	3.2	3.0	331

Relaxed Substorm Conditions (low density/high velocity)

Day	Hour	Density (#/cm^3)	Energy (eV)	Bulk Speed (km/s)
28	23	3.2	14.7	617
29	0	2.7	14.7	610
29	1	2.5	14.7	602
29	2	2.3	14.7	609
29	3	2.6	14.7	612

Measurements from the GEOTAIL [4] spacecraft's Comprehensive Plasma Instrument Hot Plasma Analyzer (CPI-HP) were used to determine the dynamic range of the solar wind in the magnetotail region. **Figure 4** shows a segment of the orbit path or the GEOTAIL spacecraft as a function of distance from the Earth in units of earth radii. The trajectory is labeled with Julian days of the year. Note that, at approximately Julian day 310 (in November 1993), the spacecraft was in the magnetotail region at ~200 earth radii. At that time, a series of substorms occurred in the tail region. Thus, this sampling should give a good measure of the solar wind parameters to be expected during extreme conditions. **Figures 5-7** plot

* The magnetotail of the magnetosphere is formed by the interactions of the solar wind with the Earth's magnetic field. In the solar direction, the magnetic field lines are compressed down to ~12 earth radii under average solar-magnetic conditions. In the anti-solar direction, the solar wind "stretches" the magnetic field lines out to hundreds of earth radii, forming the magnetotail.

the plasma density, velocity, and temperature for a 24 hour period during the substorm. A sampling of the data for that time period is given in **Table 3**. The ion composition is roughly 95%H^+ and 5% H^{++}.

Table 3
GEOTAIL Comprehensive Plasma Instrument – Hot Plasma Analyzer
Magnetotail Plasma at ~210 Re During Substorm Conditions, November 18, 1993

High Density/Low Bulk Velocity and Thermal Energy

Hour	Min	S	Density (#/cm^3)	Energy (eV)	Bulk Speed (km/s)
3	50	12.17	27.7	17.8	261.7
3	51	16.17	28.4	20.6	258.1
3	52	20.17	27.5	15.7	256.0
3	53	24.17	38.1	11.7	256.1
3	54	28.17	45.2	9.4	249.2
3	55	32.17	31.2	13.6	251.3
3	56	36.17	31.7	11.5	256.7
3	57	40.17	28.2	14.2	260.4
3	58	44.17	21.1	22.3	261.2
3	59	48.17	26.7	16.4	256.1
4	0	52.17	39.7	11.0	253.0

Low Density/High Bulk Velocity and Thermal Energy

Hour	Min	S	Density (#/cm^3)	Energy (eV)	Bulk Speed (km/s)
5	26	12.17	0.1	562.3	307.3
5	27	16.17	0.2	1043.9	331.3
5	28	20.17	0.2	724.9	276.8
5	29	24.17	0.2	1011.3	193.1
5	30	28.17	0.1	1499.4	175.2
5	31	32.17	0.1	1167.0	349.8
5	32	36.17	0.1	1047.4	519.5
5	33	40.17	0.2	642.5	360.5
5	34	44.17	0.1	848.7	369.8
	35	48.17	0.1	824.7	534.7
5	36	52.17	0.1	1333.9	258.2

A comparison of the SOHO and GEOTAIL measurements for the solar wind shows that the plasma density in the magnetotail can increase to over 100 particles/cm^3 for short periods of time (Figures 1 and 5). Comparing Figures 3 and 7, it can be seen that the energy of the plasma can increase in the magnetotail from a "few eV" to the keV level. For these samplings, the general description of the velocity as 400 km/s is accurate; however, Figure 6 shows that the solar wind velocity has a large range within a 24-hour period and that the changes are extremely rapid.

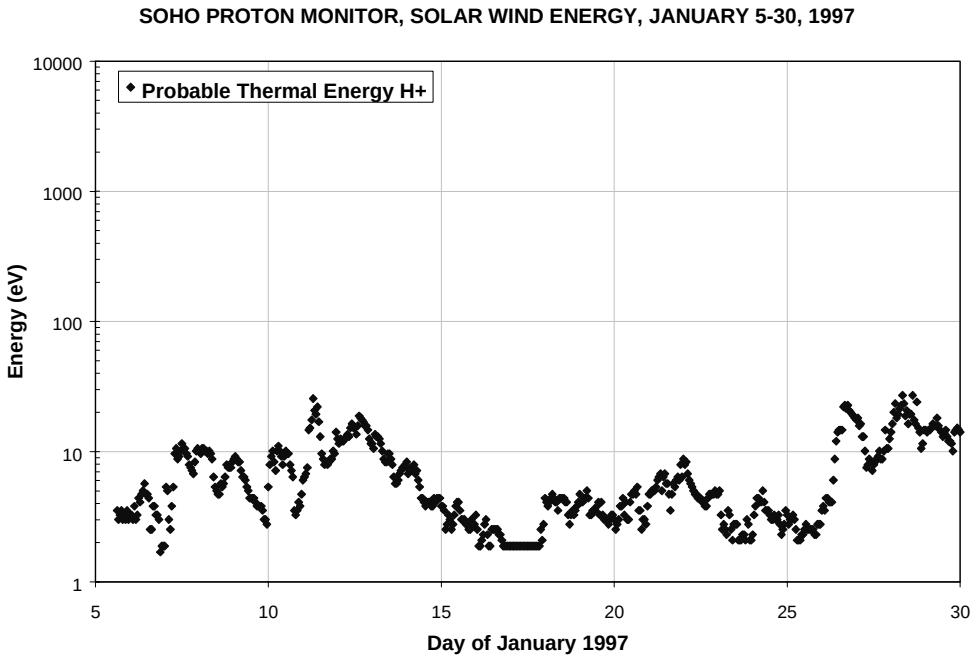

Figure 1: A sampling of the solar wind energy as measured by the SOHO spacecraft.

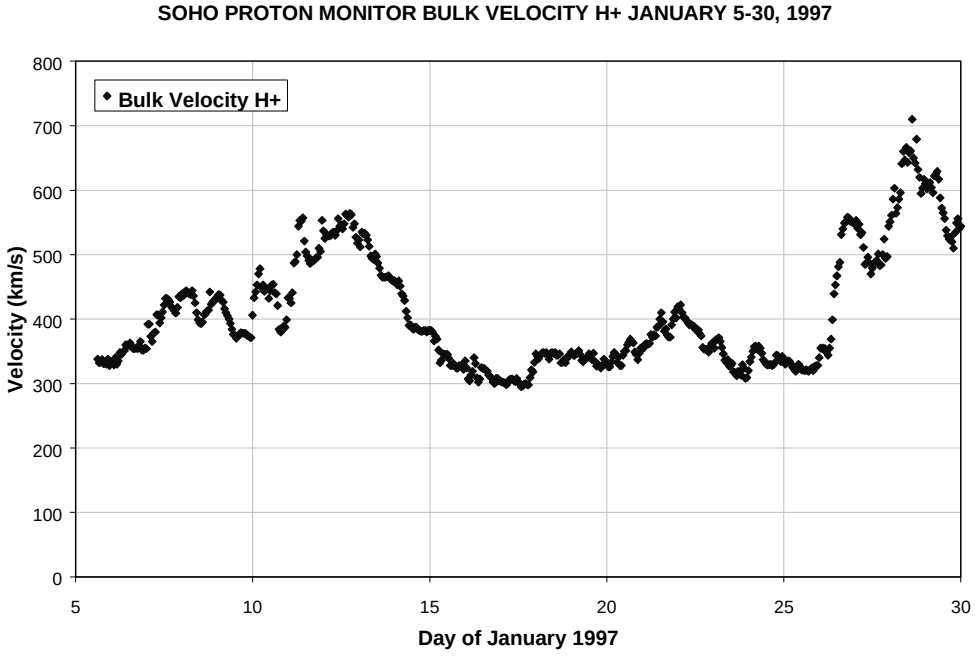

Figure 2: A sampling of the solar wind velocity as measured by the SOHO spacecraft.

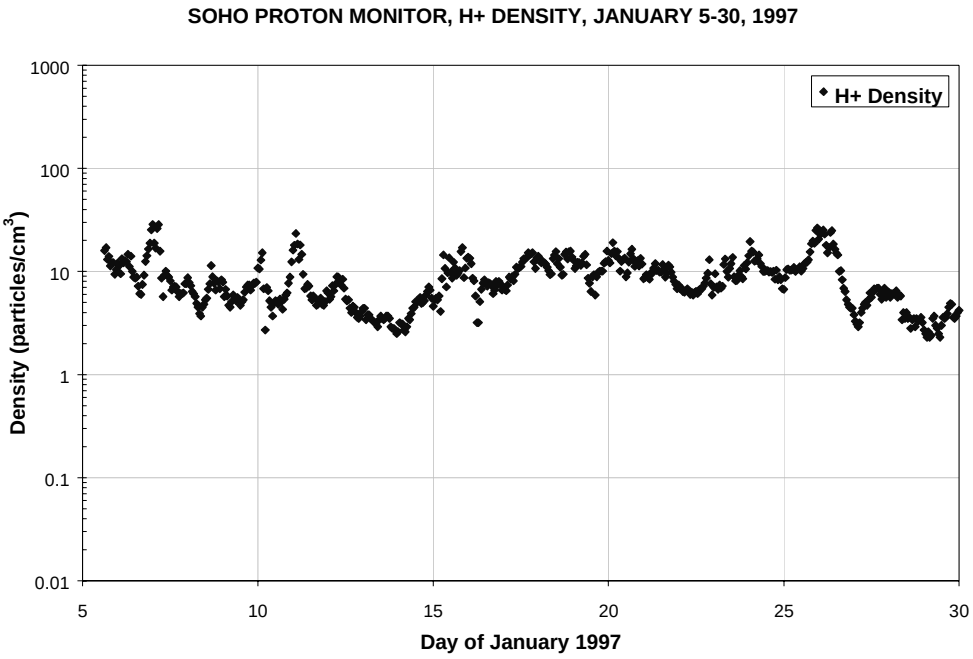

Figure 3: A sampling of the solar wind density as measured by the SOHO spacecraft.

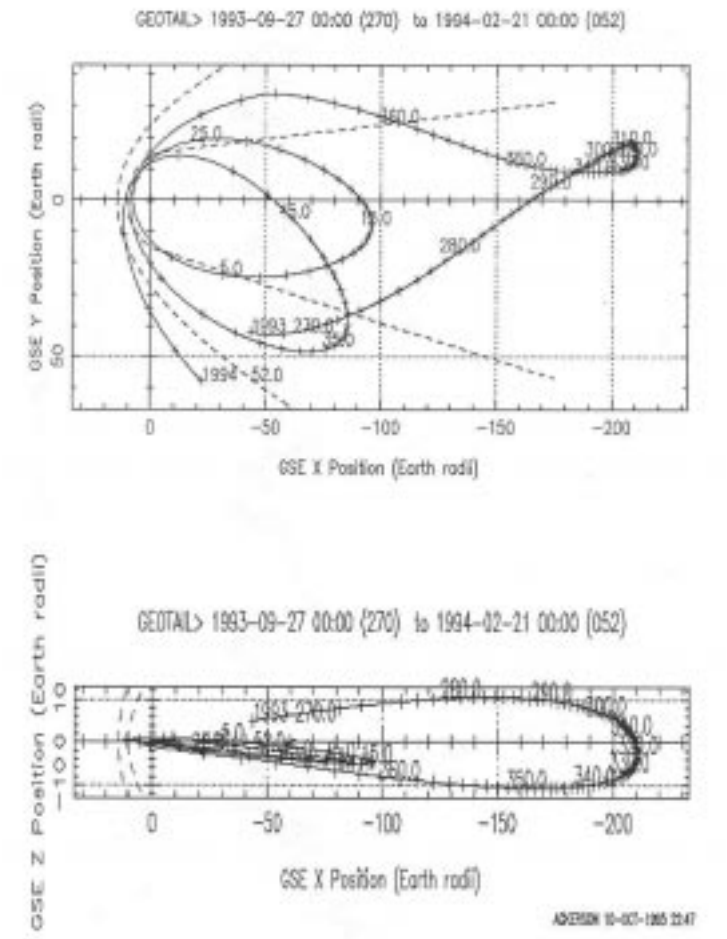

Figure 4: Position of GEOTAIL in the magnetotail.

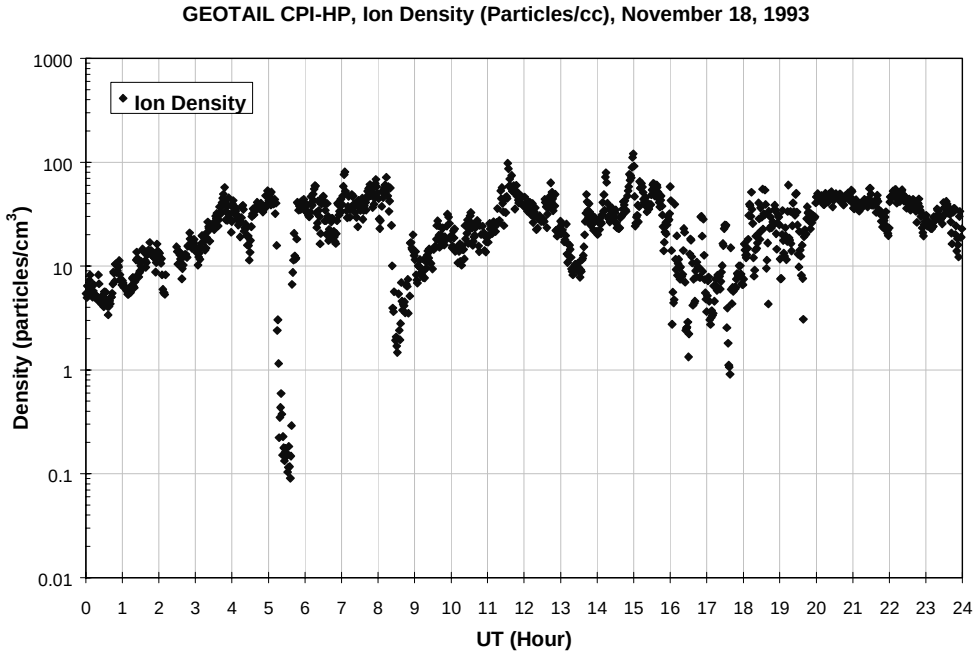

Figure 5: A sampling of the ion density as sampled by GEOTAIL.

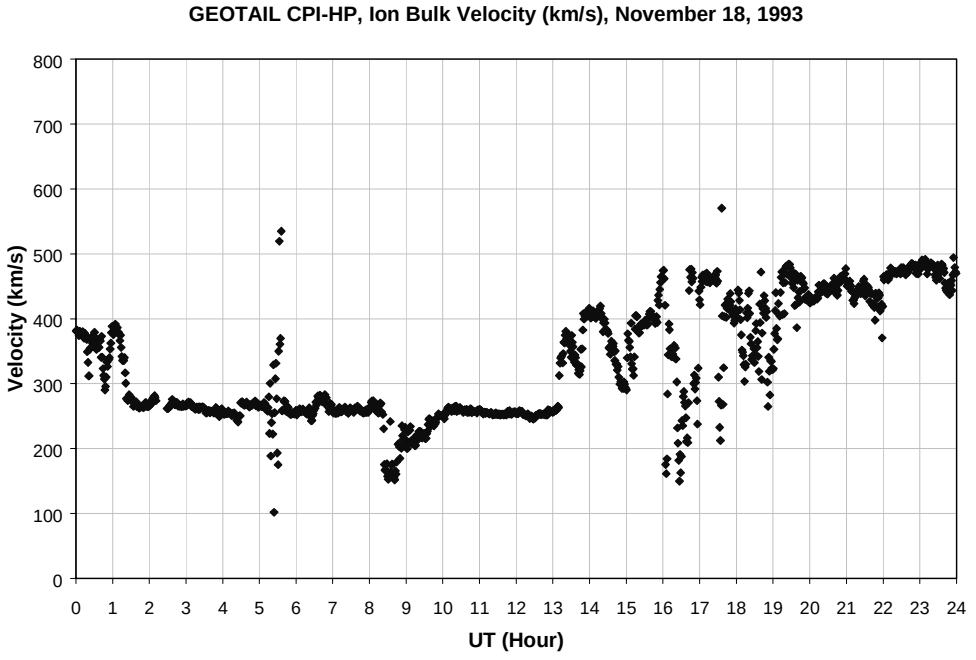

Figure 6: A sampling of ion bulk velocity by GEOTAIL.

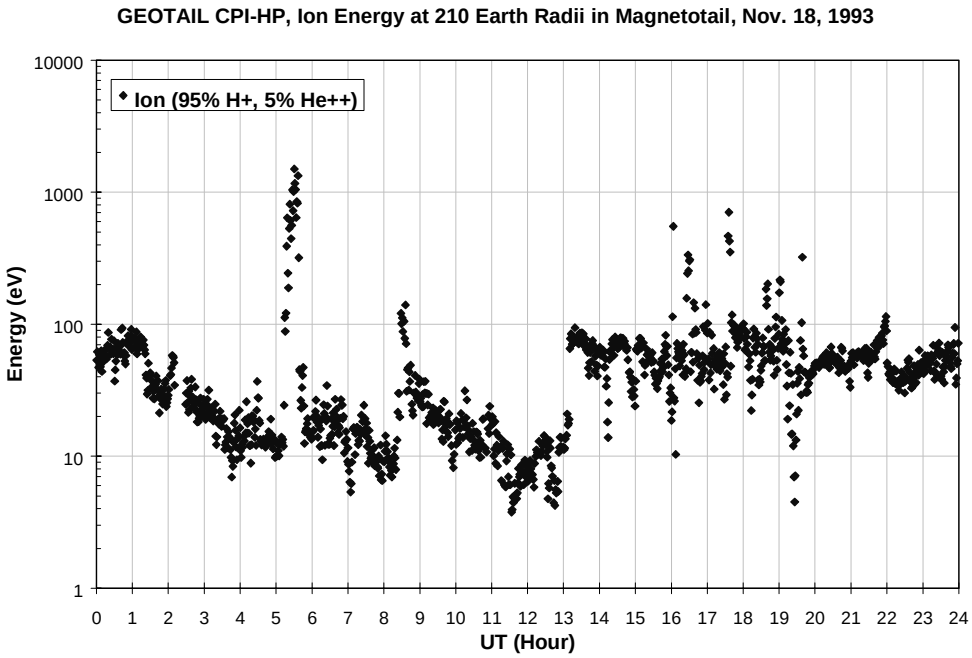

Figure 7: A sampling of ion energy by GEOTAIL.

2. High Energy Particles – Spacecraft Incident Fluences

The spacecraft incident proton fluence levels given in this document are most often used for standard solar cell analyses that take into account the coverglass thickness of the cell. There are three possible sources of high energy particles: trapped protons and trapped electrons encountered in the transfer trajectory and protons from solar events that can occur anytime during the three solar active years of the mission. The trapped particles encountered in the transfer trajectory cannot be evaluated at this time but are usually not a factor in degradation analyses. The proton fluence levels are also used to determine displacement damage effects, however, most analysis methods require that the surface incident particles be transported through the materials surrounding the sensitive components. The proton fluences behind nominal aluminum shield thicknesses are given in Section 5.B.3.

When the transfer trajectory is known, the trapped particle fluxes will be estimated with NASA's AP-8 [5] model for protons and AE-8 [6] model for electrons. The models come in solar minimum and maximum versions. The uncertainty factors defined for the models are a factor of 2 for the AP-8 and 2 to 5 for the AE-8. These uncertainty factors apply to long term averages expected over a 6 month mission duration. Daily values can fluctuate by two to three orders of magnitude depending on the level of activity on the sun and within the magnetosphere.

The solar proton levels can now be estimated from the new Emission of Solar Proton (ESP) model [7]. Previously, estimates of solar proton levels were obtained from models [8,9] that were largely empirical in nature, making it difficult to add data to the model from more recent solar cycles. The ESP model is based on satellite data from solar cycles 20, 21, and 22. The distribution of the fluences for the events is obtained from maximum entropy theory, and design limits in the worst case models are obtained from extreme value theory.

Total integral solar proton fluences were estimated for 2, 3, and 4 solar active years with 3 years being the best estimate available at this time. **Tables A1-A3** give the fluence levels as a function of particle energy

for 80, 85, 90, 95, and 99% confidence levels. **Figures 8-10** are plots of the energy-fluences spectra for 2, 3, and 4 solar active years for the given confidence levels. In addition, **Figure 11** compares the 2, 3, and 4 year solar proton fluence levels for the 95% confidence level. The energies are in units of >MeV and the fluences are in units of particles/cm^2. These values do not include a design margin. The solar proton predictions are not linear over time; therefore, these estimates may be invalid if extrapolated for longer mission durations.

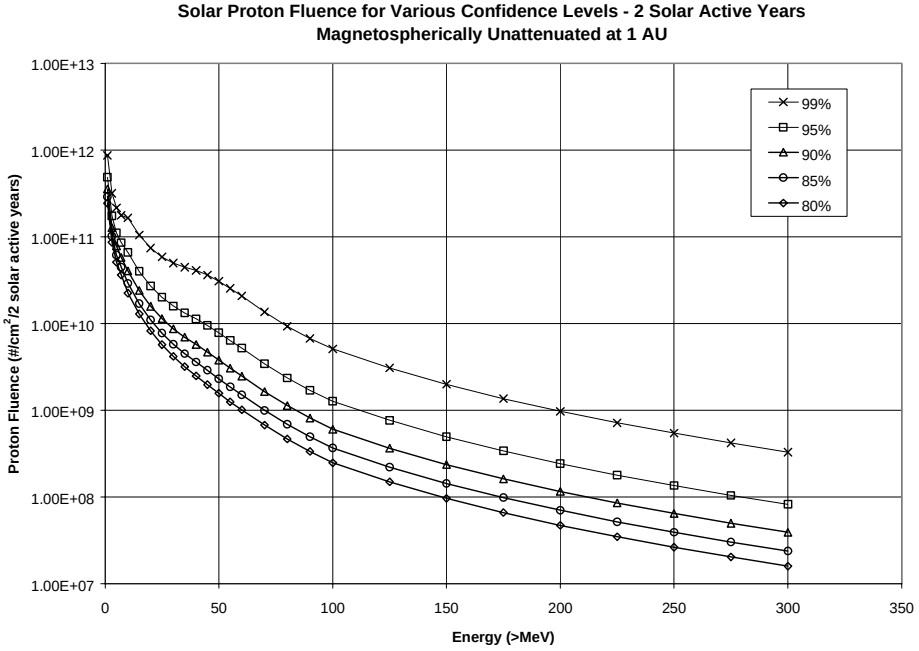

Figure 8: Solar proton fluences for 2 solar active years are presented for various confidence levels.

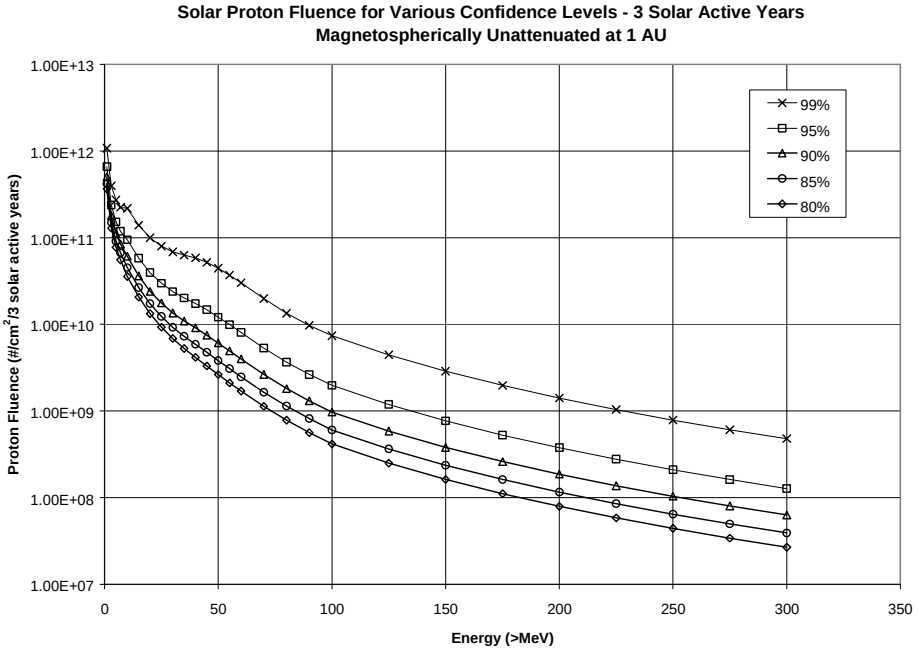

Figure 9: Solar proton fluences for 3 solar active years are presented for various confidence levels.

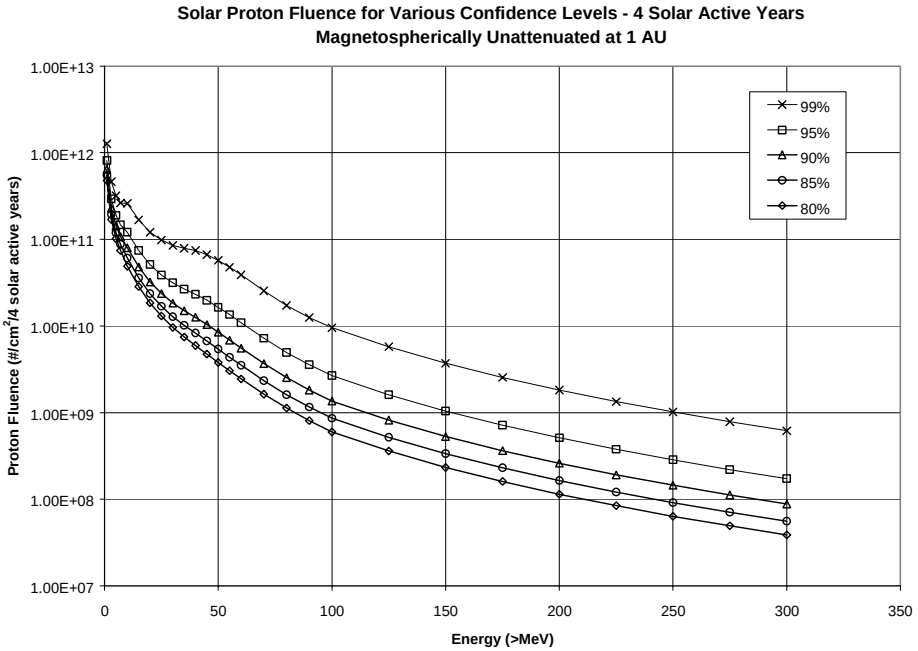

Figure 10: Solar proton fluences for 4 solar active years are presented for various confidence levels.

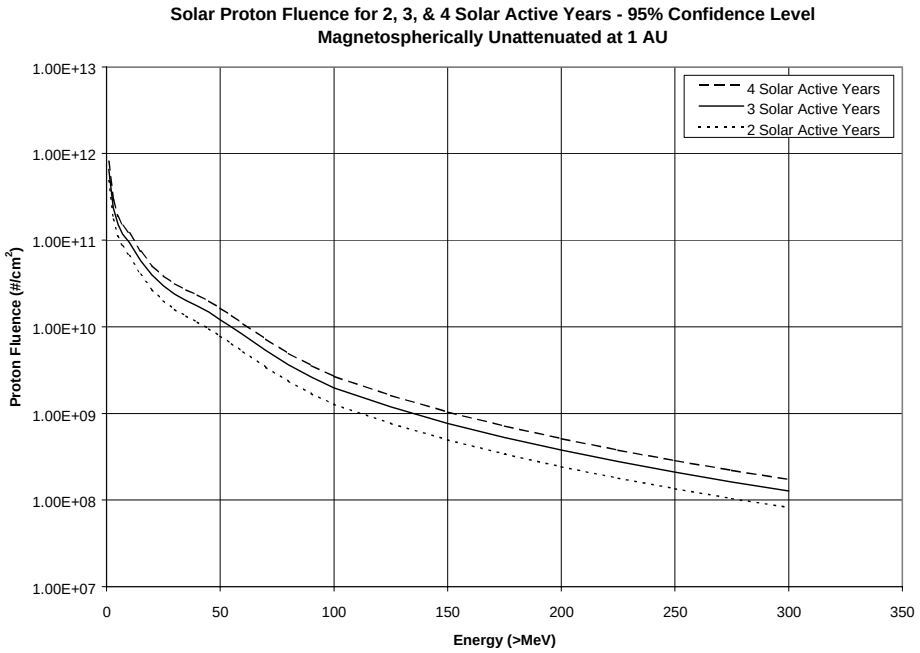

Figure 11: Solar proton fluences for a 95% confidence level are presented for 2, 3, and 4 solar active years.

3. High Energy Particles – Shielded Fluences

Evaluation of non-ionizing energy loss damage requires the use of shielded fluence levels. For this analysis nominal shielding thicknesses of 50, 100, 200, and 500 mils of aluminum were used for a generic solid sphere geometry. The spacecraft incident, solar proton estimates for the 95% confidence level and for 2, 3, and 4 year solar active years were transported through the shield thickness to obtain fluence estimates behind the shielding. **Tables A4-A6** give the degraded energy spectra. The spectra are plotted in **Figures 12-14**. **Figure 15** shows a comparison for 2, 3, and 4 solar active years for 100 mil shielding case. It can be seen from the figures that even though low energy particles are absorbed by the shielding, the low energy range of the spectrum is filled in by the higher energy protons as they are degraded by passing through the material.

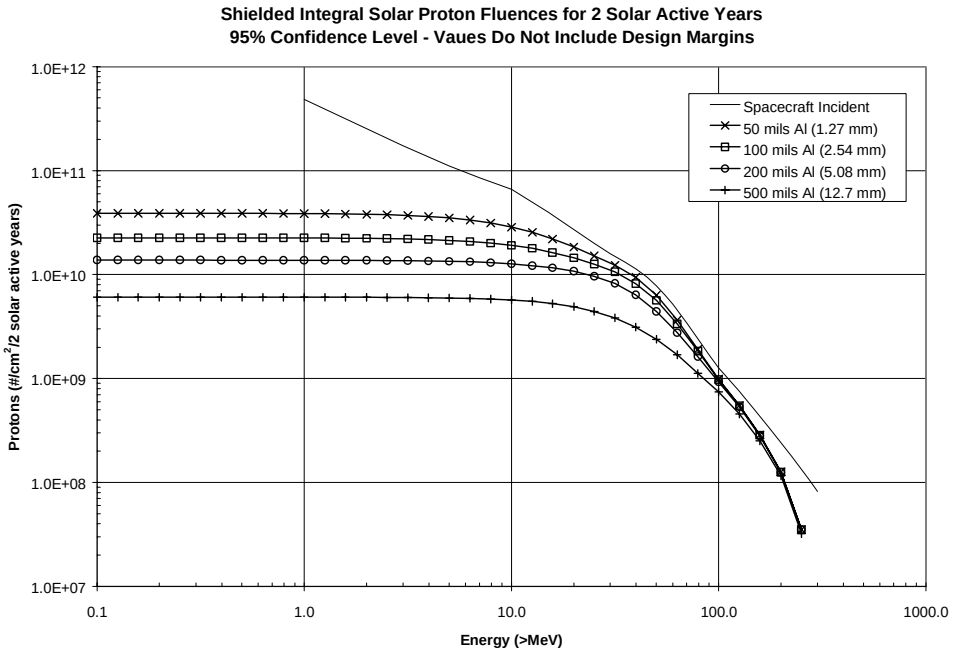

Figure 12: Shielded solar proton energy spectra for 2 solar active years, 95% confidence level.

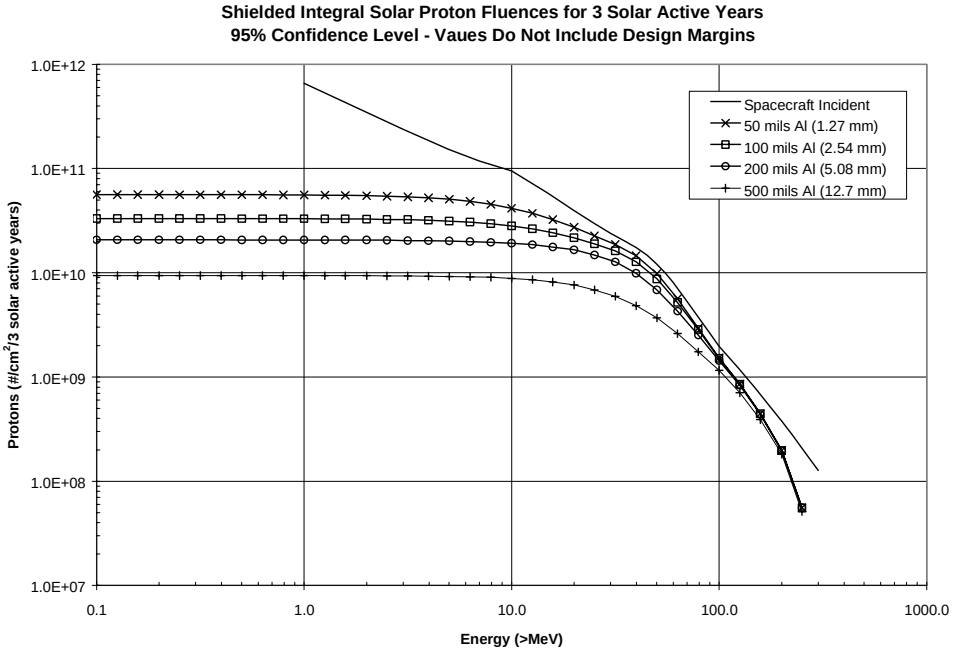

Figure 13: Shielded solar proton energy spectra for 3 solar active years, 95% confidence level.

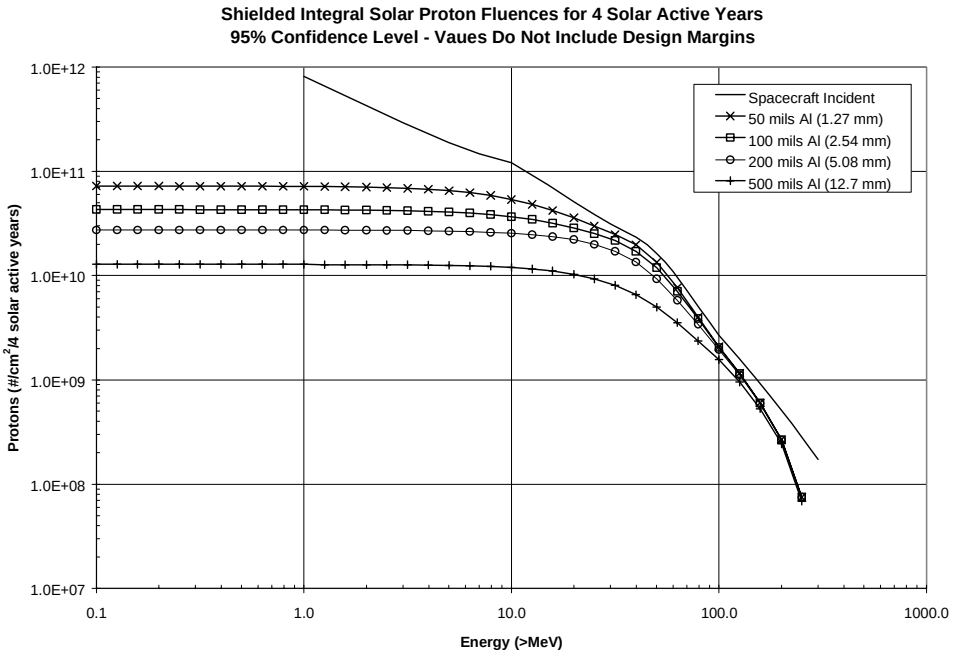

.

.

...

Figure 14: Shielded solar proton energy spectra for 4 solar active years, 95% confidence level.

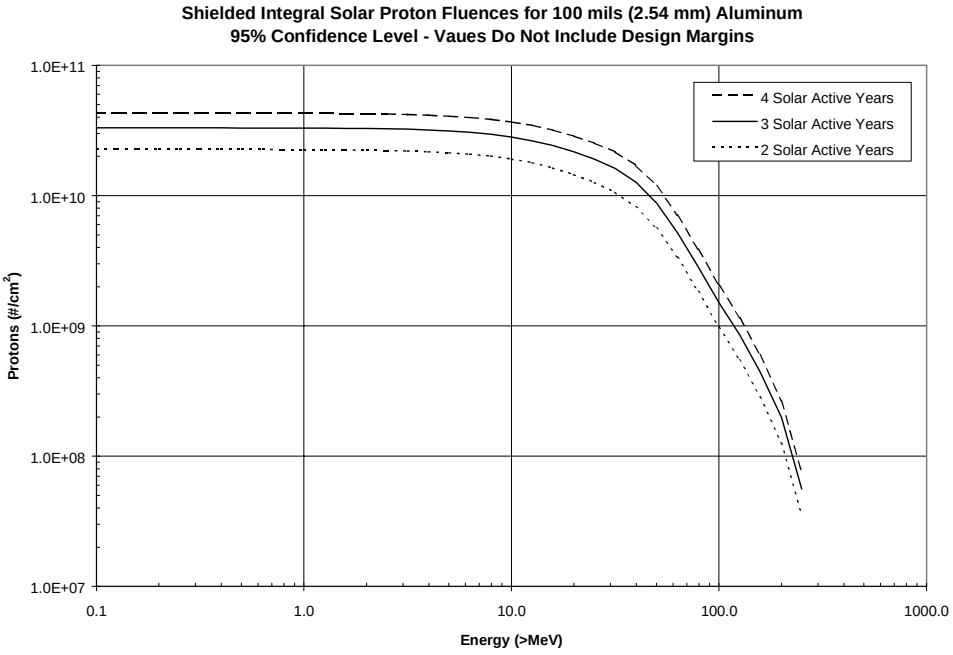

Figure 15: Shielded solar proton energy spectra for 100 mils aluminum 95% confidence level

B. Total Dose Estimates

1. Top Level Ionizing Dose Requirement

Doses are calculated from the surface incident integral fluences as a function of aluminum shield thickness for a simple geometry. The geometry model used for spacecraft applications is the solid sphere. The solid sphere doses represent an upper boundary for the dose inside an actual spacecraft and are used as a top-level requirement. In cases where the amount of shielding surrounding a sensitive location is difficult to estimate, a more detailed analysis of the geometry of the spacecraft structure may be necessary to evaluate the expected dose levels. This is done by modeling the electronic boxes or instruments and the spacecraft structure. The amount of shielding surrounding selected sensitive locations is estimated using solid angle sectoring and 3-dimensional ray tracing. Doses obtained by sectoring methods must be verified for 5-10% of the sensitive locations with full Monte Carlo simulations of particle trajectories through the structure for many histories.

Table A7 and **Figures 16** and **17** give the top-level total ionizing dose requirement for the 5 year NGST mission. Because of the uncertainty in the length of the solar cycle, the doses are given for 2, 3, and 4 solar active years for a 95% confidence level. The best estimate at this time predicts 3 solar active years given the 2008 NGST launch. The doses are calculated here as a function of aluminum shield thickness in units of krads in silicon. For the nominal 100 mils of equivalent aluminum shielding and worst case 4 years of solar activity, the dose requirement is 15 krads-si with no design margin. A minimum design margin of x 2 is recommended.

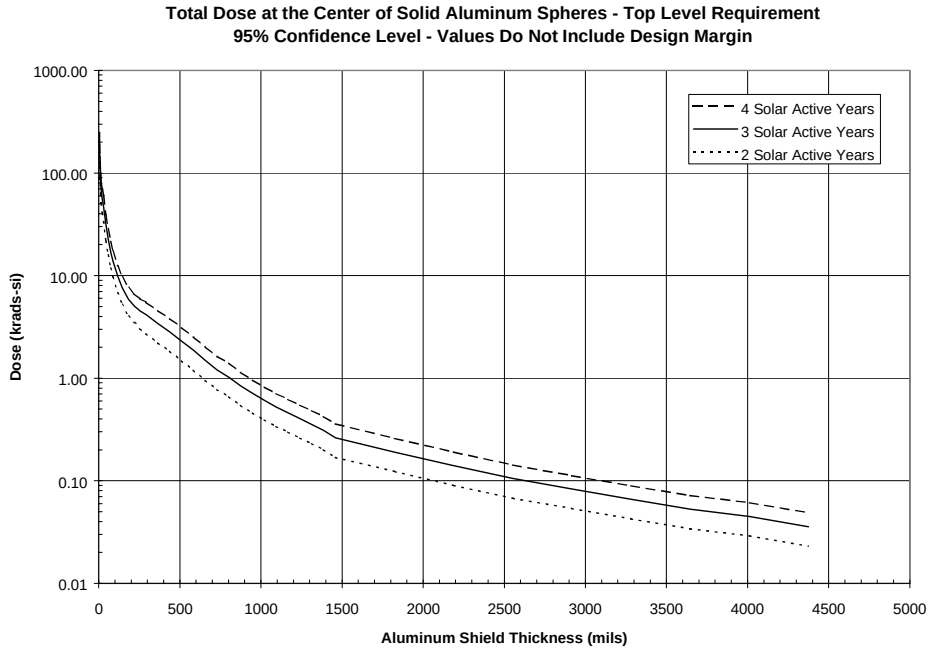

Figure 16: Total ionizing dose from solar proton events for 2, 3, and 4 solar active years is presented.

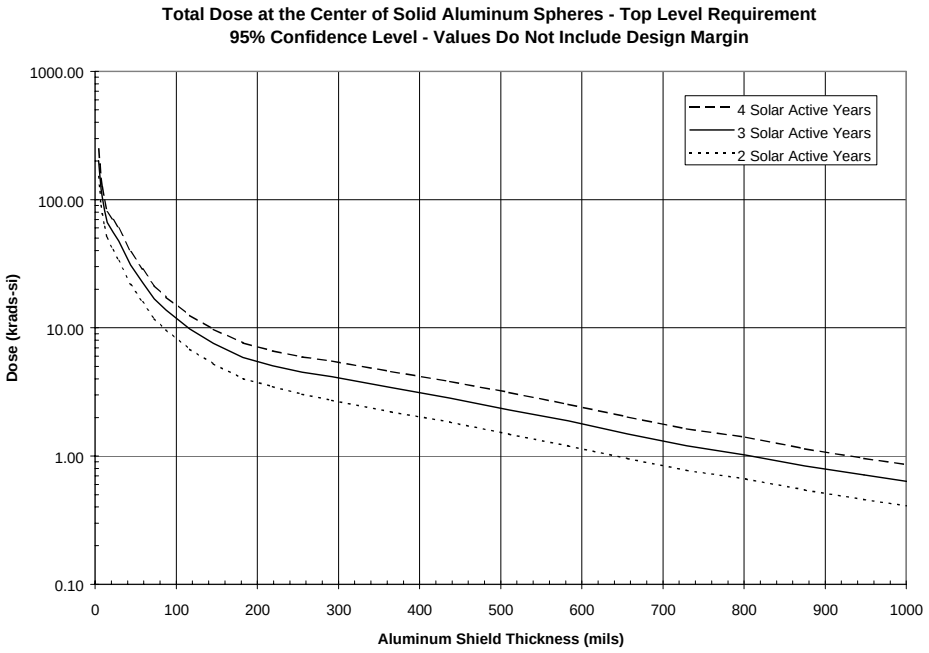

Figure 17: Total ionizing dose from solar proton events for 2, 3, and 4 solar active years is presented.

2. Dose at Specific Spacecraft Locations

In cases where parts cannot meet the top level design requirement and a "harder" part cannot be substituted, it is often beneficial to employ more accurate methods of determining the dose exposure for some spacecraft components to qualify the parts. One such method for calculating total dose, solid angle sectoring/3-dimensional ray tracing, is accomplished in three steps:

1) Model the spacecraft structure:
   -develop a 3-D model of the spacecraft structures and components
   -develop a material library
   -define sensitive locations
2) Model the radiation environment:
   -define the spacecraft incident radiation environment
   -develop a particle attenuation model using theoretical shielding configurations (similar to dose-depth curves).
3) Obtain results for each sensitive location:
   -divide the structural model into solid angle sectors
   -ray trace through the sectors to calculate the material mass distribution
   -use the ray trace results to calculate total doses from the particle attenuation model.

Once the basic structural model has been defined, total doses can be obtained for any location in the spacecraft in a short time (in comparison to Monte Carlo methods). The value of dose mitigation measures can be accurately evaluated be adding the changes to the model and recalculating the total dose. For

spacecraft with strict weight budgets, the 3-D ray trace method, the total dose design requirement can be defined at a box or instrument level avoiding unnecessary use of expensive or increasingly unavailable radiation hardened parts.

As the design of the NGST evolves, it may become necessary to estimate the doses at specific locations in the spacecraft or instruments. Often the dose requirement can be met by modeling the surrounding electronic box only or by modeling only the instrument.

C. Displacement Damage Estimates

Total non-ionizing energy loss damage is evaluated by combining the shielded proton energy spectra given Section V.A.3 with the NEIL response curves for the material and the results of laboratory radiation of the devices sensitive to atomic displacement damage. The level of the hazard is highly dependent on the device type and can be process specific. For the NGST mission, it is important to keep in mind that some optoelectronic devices experience enough damage during one large solar proton event to cause the device to fail. It is necessary that the parts list screening for radiation also include a check for devices that are susceptible to displacement damage.

VI. Single Event Effects Analysis

A. Heavy Ion Induced Single Event Effects

Some electronic devices are susceptible to single event effects (SEEs), e.g., single event upsets, single event latch-up, single event burn-out. Because of their ability to penetrate to the sensitive regions of devices and their ability to ionize materials, heavy ions cause SEEs by the direct deposit of charge. The quantity most frequently used to measure an ion's ability to deposit charge in devices is linear energy transfer (LET). Heavy ion abundances are converted to total LET spectra. Once specific parts are selected for the mission and, if necessary, characterized by laboratory testing, the LET spectra for the heavy ions are integrated with the device characterization to calculate SEE rates. Heavy ion populations that have sufficient numbers to be a SEE hazard are the galactic cosmic rays and those from solar events.

1. Galactic Cosmic Rays

The cosmic ray fluxes for elements hydrogen through uranium were used to calculate daily LET spectra for 100 mils nominal aluminum shielding as given in **Table A8** and **Figure 18**. The range of the cosmic ray abundances is bounded by the extremea of the solar active and inactive phases of the solar cycle with the highest values occurring during the solar inactive phase and the lowest during the solar active phase. With the mission goal of 10 years, the highest values should be used for single event effects analyses. The LET fluence values are given for the highest and lowest point of the solar cycle. The new CREME96 [10] model was used to obtain the cosmic ray heavy ion abundances. This model has an accuracy of 25-40%.

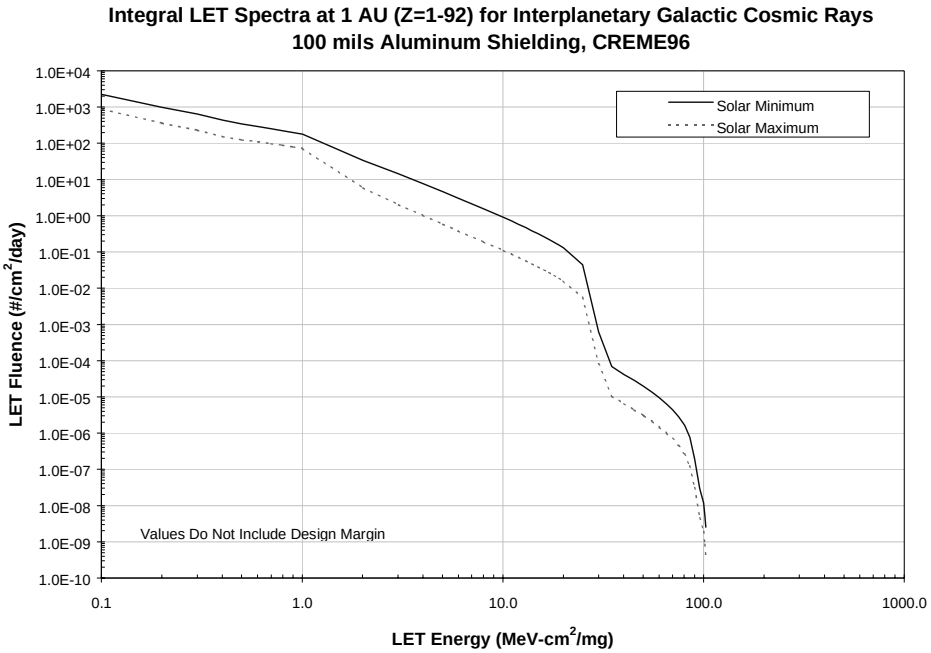

Figure 18: Integral LET spectra are shown for galactic cosmic ray ions hydrogen through uranium.

2. Solar Heavy Ions

The heavy ions from solar flares and coronal mass ejections can also produce single event effects. The solar event fluxes for the elements hydrogen through uranium were used to calculate daily LET spectra for 100 mils nominal aluminum shielding in units of average LET flux per second. The intensity of the fluxes varies over the duration of an event; therefore, values are averaged over the worst week of the solar cycle, the worst day of the solar cycle, and the peak of the October 1989 solar event. **Table A9** and **Figure 19** give the solar heavy ion LET predictions for the NGST mission. The new CREME96 model was also used to calculate the solar heavy ion levels. An uncertainty factor for the solar heavy ion model has not been released.

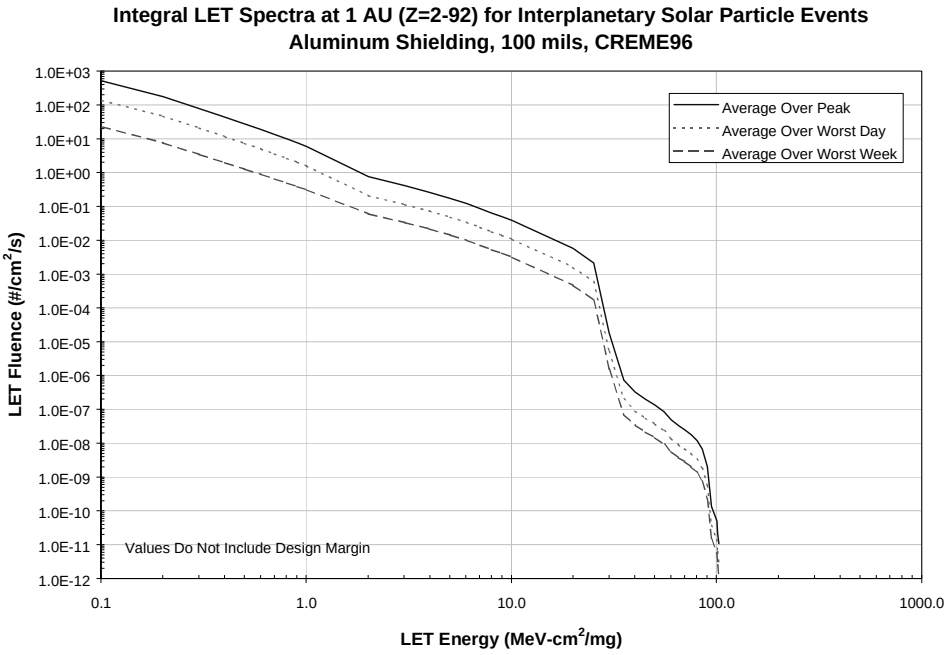

Figure 19: Integral LET spectra are shown for hydrogen through uranium for the October 1989 solar particle event.

B. Proton Induced Single Event Effects

In some devices, single event effects are also induced by protons. Protons from the trapped radiation belts and from solar events do not generate sufficient ionization (LET < 1 MeV-cm^2 /mg) to produce the critical charge necessary for SEEs to occur in most electronics. More typically, protons cause secondary effects through nuclear interactions, that is, spallation and fractionation products. Because the proton energy is important in the production (and the LET) of the secondary particles that cause the SEEs, device sensitivity to these particles is typically expressed as a function of proton energy rather than LET.

1. Trapped Protons

Trapped protons can be a concern for single event effects during the transfer trajectory passes through the trapped particle radiation belts. The proton fluxes in the intense regions of the belts reach levels that are high enough to induce upsets or latchups. The timing of critical operations during the transfer trajectory should be analyzed to determine the trapped proton environment at the time of the operation.

2. Solar Protons

Protons from solar events can also be a single event effects hazard for the NGST spacecraft. These enhanced levels of protons could occur anytime during the 5-year mission but are most likely during the portion of the mission that occurs during the active phase of the solar cycle. As with the solar heavy ion LET, solar proton fluxes are averaged over worst day, worst week, and the peak of the October 1989 solar event. The proton flux averages for a nominal 100 mils of shielding are given in **Table A10** and are shown in **Figure 20**.

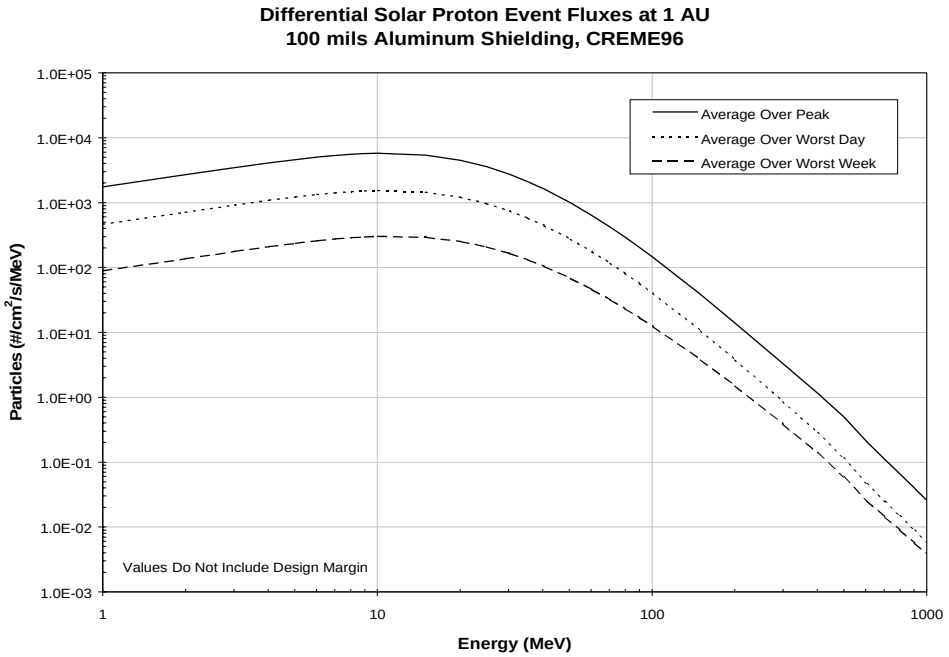

Figure 20: Solar proton fluxes for single event effects evaluation.

VII. Instrument Interference

For NGST the particle background is also a concern for instrument observations. To estimate the nominal particle background level, the energy spectra for galactic cosmic ray heavy ion elements were estimated with the CREME96 model and summed. Fifty mils of aluminum shielding was assumed. The result is shown in **Figure 21**. Note that the hydrogen component dominates the total number of ions. The total ion flux was integrated over energy to obtain a background count of 5 ions/cm^2/s.

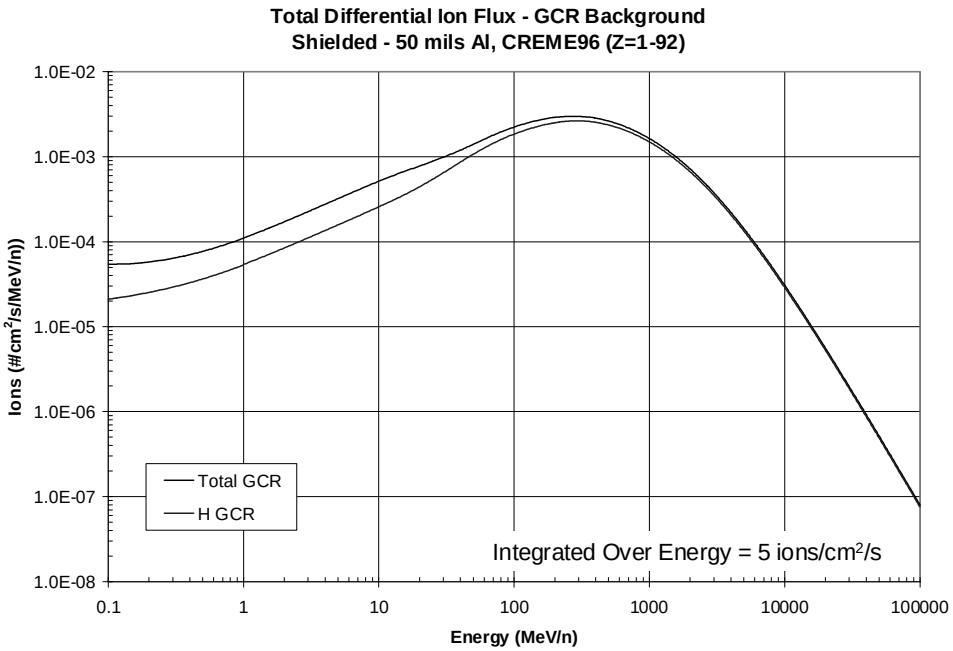

Figure 21: Total differential fluence for all galactic cosmic ray particles for a 1 second time period.

Particle interference during solar events is of particular concern because it can impact the observation times of the instruments. To obtain an estimate for the peak particle count, the total number of particles was estimated from the solar heavy ion model of the CREME96 code which is based on the October 1989 solar particle event. The particles were summed and integrated using the same method as with the galactic cosmic ray background. It was estimated the particle rate is approximately 2.5 x 10^5 ions/cm^2/s. The results are shown in **Figure 22**.

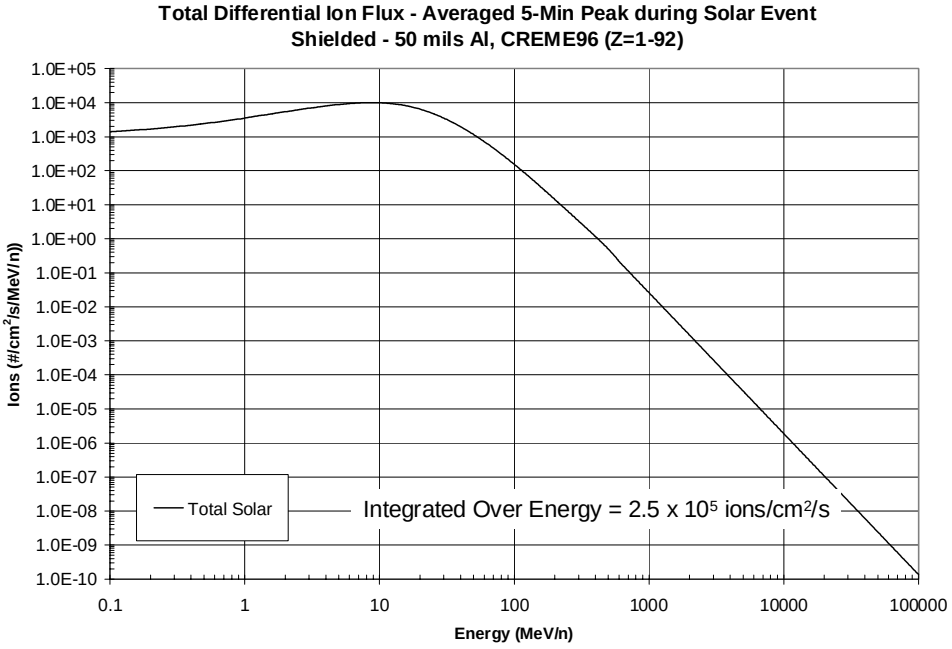

Figure 22: Total differential fluence of all predicted solar particles based on the October 1989 event

It is necessary to have a clearer understanding of how the solar particle events impact viewing and data collection activities on the NGST. Therefore, solar proton flux data were obtained from the Space Environment Monitor (SEM) Mission of the Geosynchronous Operational Environmental Satellites (GOES) [11]. The 5 minute average data were extracted from the GOES SEM data base* and converted to integral flux in particles/cm^2/s/steradian for proton flux levels greater than 1, 5, 10, 30, 50, 60 and 100 MeV, for the years 1986 through 1996. These data were converted to hourly averages in order to reduce the size of the data set.

The distribution of solar proton flux for particles with energies greater than 30 and 50 MeV were first analyzed. The distribution is measured by counting the number of hours the average flux was greater than 1, 2, 5, 10, 20, or 50 particles/cm^2/s for each year, and converting hours to days for presentation purposes. The results are shown in **Figures 23** and **24**.

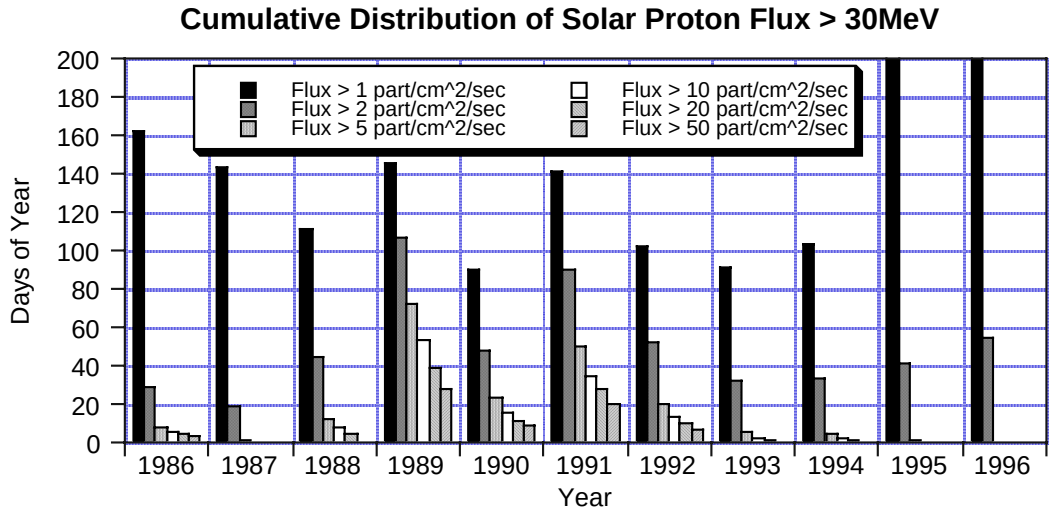

Figure 23: The cumulative distribution of > 30 MeV solar protons for the last solar cycle.

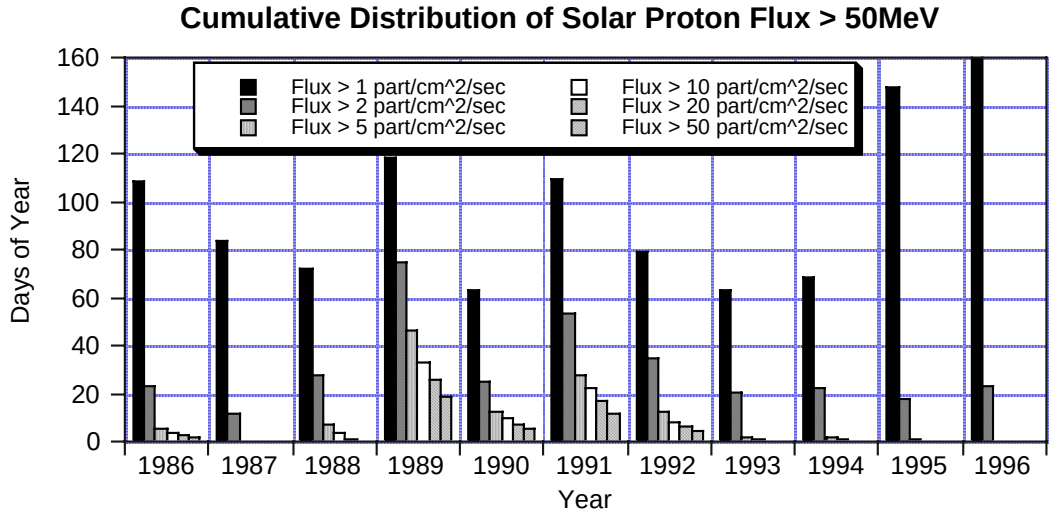

* The authors wish to thank Paul McNulty and Craig Stauffer of SGT, Inc., Greenbelt, MD for their support in extracting the GOES data.

Figure 24: The cumulative distribution of > 50 MeV solar protons for the last solar cycle

These figures clearly show the impact of most active periods of the solar maximum phase solar cycle 22, which occurred during the years 1989-1992. If solar cycle 24 has a period of 11 years and its activity is similar to solar cycle 22, the peak of the solar particle activity will occur during the years 2011-2014 following NGST launch around 2008.

Extreme flux levels will raise the concern of single event upsets interfering with operation of the vehicle or posing a health and safety hazard. To establish reasonable worst case scenarios for the solar radiation environment, the next analysis focused on the years 1989-1991. **Figures 25-27** show the hourly average solar proton flux for particles greater than 50 MeV for each of the years 1989-1991. Note that the scale for flux is logarithmic, and the flux variation is significant.

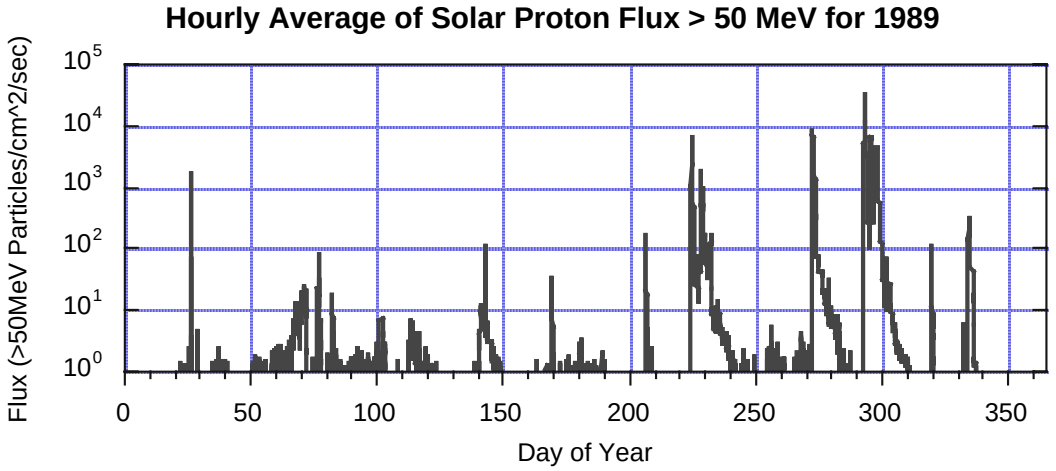

Figure 25: Hourly averages of solar proton fluxes for > 50 MeV protons for 1989.

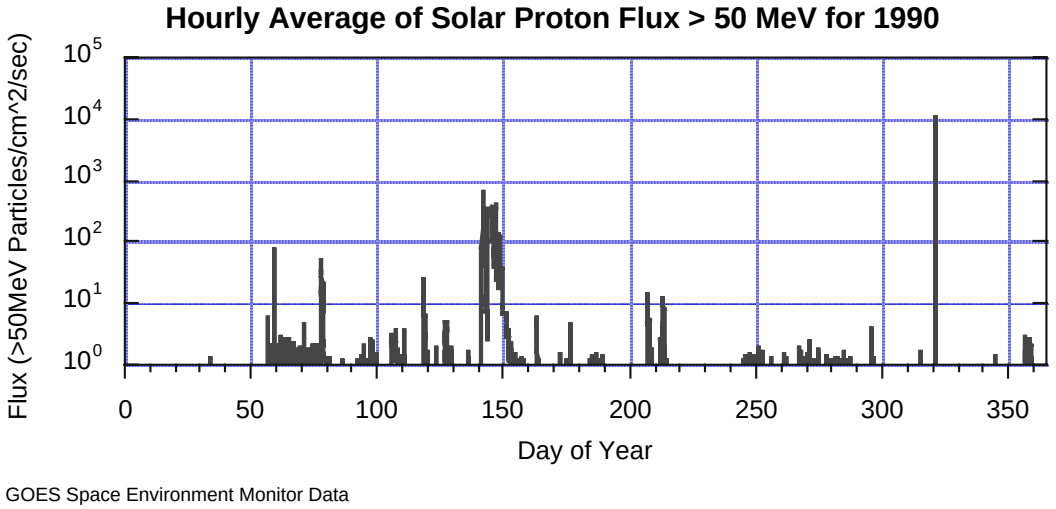

Figure 26: Hourly averages of solar proton fluxes for > 50 MeV protons for 1990.

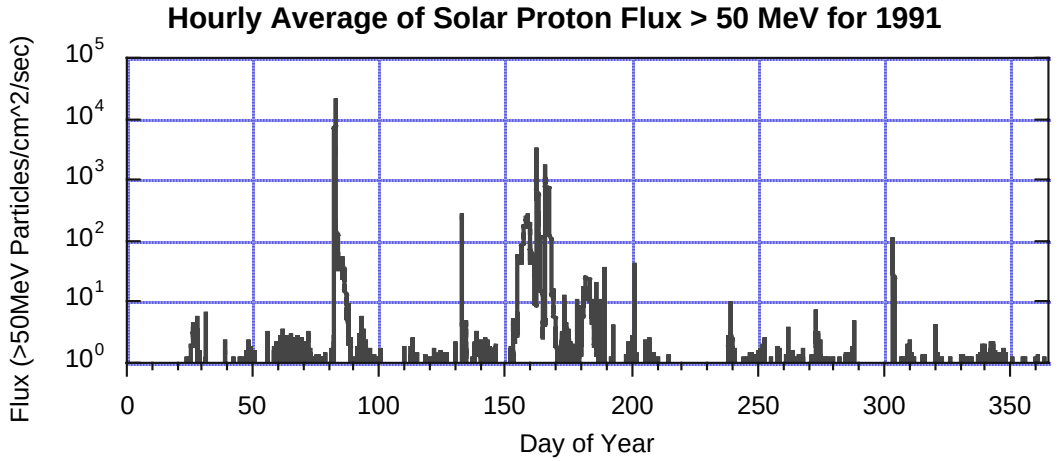

Figure 27: Hourly averages of solar proton fluxes for > 50 MeV protons for 1991.

Moderate flux levels will affect the ability of NGST to observe dim targets with long exposures. The galactic background flux is 5 particles/cm^2/s at L2, so NGST will be configured to operate in this environment. To address the problem of observation interference during solar particle events, the distributions of the solar proton flux counts for 1989, 1990, and 1991 were estimated. During these solar maximum years, the solar proton flux will vary significantly and will increase the total flux by several particles for a large portion of the year. **Figures 28** and **29** show the cumulative distributions of solar proton flux for particles greater than 30 and 50 for 1989, 1990, and 1991, and the average of these years.. These figures show that, for an average of almost two months for each year of solar maximum, the solar proton flux will exceed 5 particles/cm^2/s for > 30 MeV protons (or over one month per year for > 50 MeV protons).

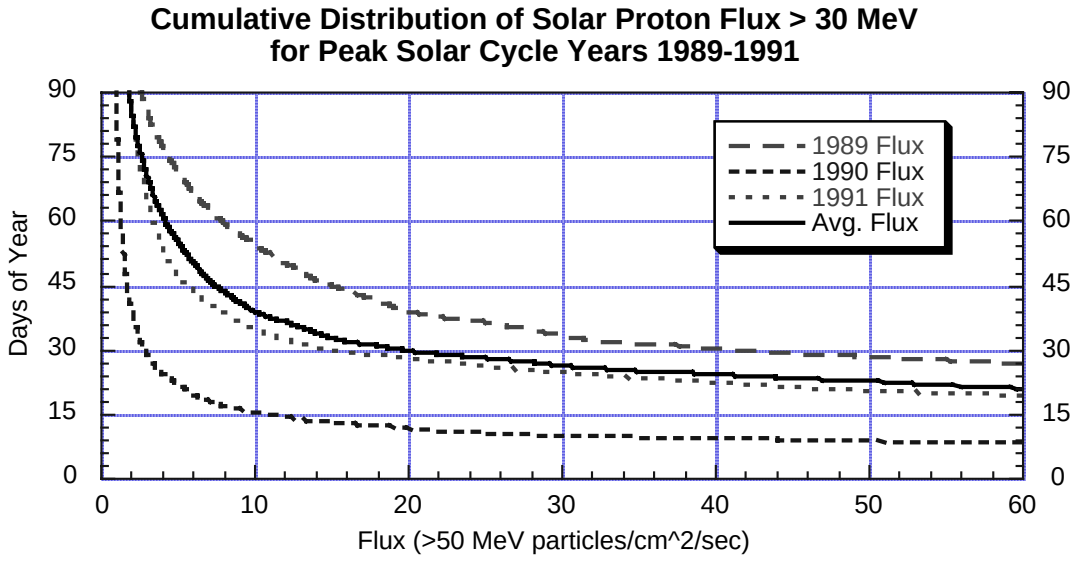

Figure 28: Distribution of solar proton flux counts at > 30 MeV

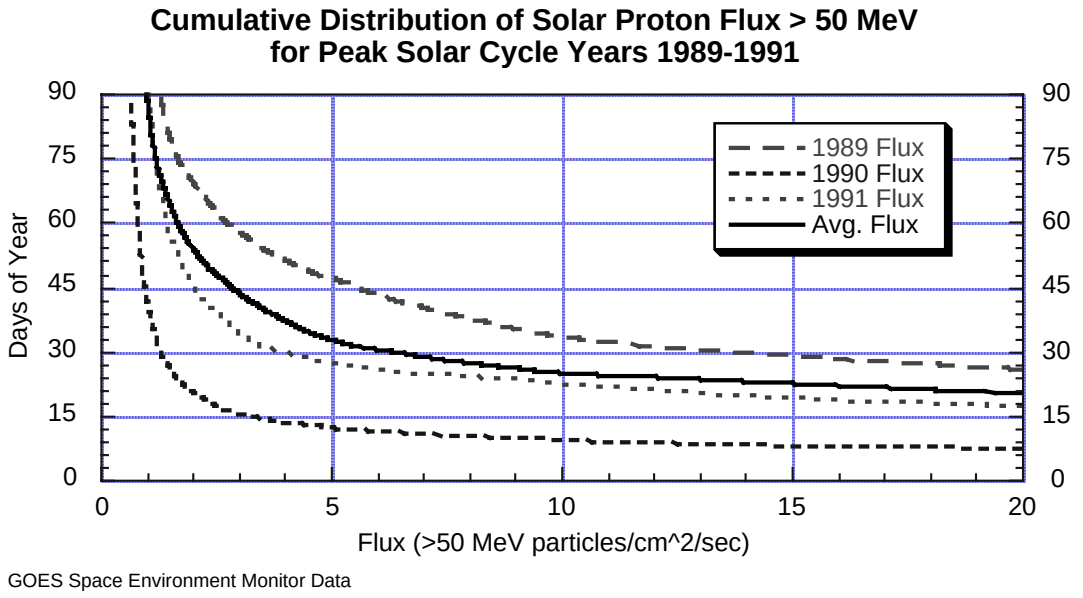

Figure 29: Distribution of solar proton flux counts at > 50 MeV.

VIII. Spacecraft Charging and Discharging

Surface charging and deep dielectric charging must also be evaluated for the NGST mission. Both are potentially a problem in transfer trajectories that take long loops through the Van Allen belts. During these loops, the spacecraft can accumulate high levels of electron build-up on spacecraft surfaces (low energy electrons) in the dielectrics (high energy electrons). When the transfer trajectory of NGST is known in more detail, the particle accumulation profiles must be estimated and analyzed for possible surface and deep dielectric charging effects.

At L2 there is also concern that surface charges can build up due to the differential in the plasma during the passes in and out of the magnetotail. This analysis should be performed when the plasma model becomes available.

IX. Summary

A top-level radiation environment specification was presented for the NGST mission. Although the environment is considered "moderate", the environment poses challenges to mission designers because of its highly variable nature caused by activity on the sun.

Spacecraft and instrument designers must be made aware that some newer technologies and commercial-off-the-shelf (COTS) devices are very soft to radiation effects. COTS devices that lose functionality at 5 krads of dose are not uncommon. One extremely large solar proton event can cause enough displacement damage degradation in some optocoupler devices to cause failure. Increasingly, single event effects require careful part selection and mitigation schemes. With its full exposure to galactic cosmic heavy ions and particles from solar events, NGST must have a carefully planned radiation engineering program.

X. References

[1] A. Holmes-Siedle and L. Adams, Handbook of Radiation Effects, p. 16, Oxford University Press, Oxford, 1993.

[2] A. R. Frederickson, "Upsets Related to Spacecraft Charging," IEEE Trans. on Nucl. Science, Vol. 43, No. 2, pp. 426-441, April 1996.

[3] F.M. Ipavich *et al.*, (in press JGR 1997), Space Physics Group, University of Maryland, "The Solar Wind Proton Monitor on the SOHO Spacecraft," [WWW Dosument], URL http://umtof.umd.edu/papers/pml.htm

[4] L. A. Frank, *et al.*, "The Comprehensive Plasma Instrumentation (CPI) for the GEOTAIL Spacecraft," J. Geomag. Geoelec., Vol. 46, pp. 23-37, 1994.

[5] D. M. Sawyer and J. I. Vette, "AP-8 Trapped Proton Environment," NSSDC/WDC-A-R&S 76-06, NASA/Goddard Space Flight Center, Greenbelt, MD, December 1991.

[6] J. I. Vette, "The AE-8 Trapped Electron Model Environment," NSSDC/WDC-A-R&S 91-24, NASA/Goddard Space Flight Center, Greenbelt, MD, November 1991.

[7] M. A. Xapsos, J. L. Barth, E. G. Stassinopoulos, G. P. Summers, E.A. Burke, G. B. Gee, "Model for Prediction of Solar Proton Events", to be published in Proceedings of the 1999 Space Environment and Effects Workshop, Farnborough, UK.

[8] E. G. Stassinopoulos, "SOLPRO: A Computer Code to Calculate Probabilistic Energetic Solar Flare Protons," NSSDC 74-11, NASA/Goddard Space Flight Center, Greenbelt, MD, April 1975.

[9] J. Feynman, T. P. Armstrong, L. Dao-Gibner, and S. Silverman, "New Interplanetary Proton Fluence Model," J. Spacecraft, Vol. 27 No. 24, pp 403-410, July-August 1990.

[10] A. J. Tylka, J. H. Adams, Jr., P. R. Boberg, W. F. Dietrich, E.O. Flueckiger, E.L. Petersen, M.A. Shea, D.F. Smart, and E.C. Smith, "CREME96: A Revision of the Cosmic Ray Effects on Micro-Electronics Code: to be published in IEEE Trans. On Nuc. Sci., December 1997.

[11] GOES home page - http://julius.ngdc.noaa.gov:8080/production/html/GOES/index.html

Appendices

Table A1
Spacecraft Incident Solar Proton Fluences for 2 Solar Active Years
Values Do Not Include Design Margins

Energy	**Confidence Level**				
(>MeV)	80%	85%	90%	95%	99%
1	2.44E+11	2.89E+11	3.56E+11	4.85E+11	8.68E+11
3	8.62E+10	1.02E+11	1.27E+11	1.74E+11	3.17E+11
5	5.09E+10	6.16E+10	7.82E+10	1.11E+11	2.16E+11
7	3.62E+10	4.46E+10	5.79E+10	8.54E+10	1.77E+11
10	2.24E+10	2.91E+10	4.05E+10	6.61E+10	1.66E+11
15	1.29E+10	1.70E+10	2.40E+10	4.01E+10	1.05E+11
20	8.24E+09	1.10E+10	1.58E+10	2.71E+10	7.42E+10
25	5.71E+09	7.75E+09	1.14E+10	2.01E+10	5.87E+10
30	4.17E+09	5.77E+09	8.68E+09	1.59E+10	4.97E+10
35	3.17E+09	4.49E+09	6.95E+09	1.33E+10	4.46E+10
40	2.49E+09	3.60E+09	5.72E+09	1.13E+10	4.10E+10
45	1.97E+09	2.89E+09	4.67E+09	9.51E+09	3.62E+10
50	1.57E+09	2.31E+09	3.78E+09	7.84E+09	3.07E+10
55	1.25E+09	1.86E+09	3.06E+09	6.40E+09	2.55E+10
60	1.01E+09	1.50E+09	2.47E+09	5.18E+09	2.08E+10
70	6.72E+08	9.97E+08	1.64E+09	3.43E+09	1.36E+10
80	4.65E+08	6.89E+08	1.13E+09	2.35E+09	9.27E+09
90	3.35E+08	4.96E+08	8.14E+08	1.70E+09	6.72E+09
100	2.47E+08	3.67E+08	6.05E+08	1.27E+09	5.09E+09
125	1.49E+08	2.21E+08	3.65E+08	7.65E+08	3.07E+09
150	9.62E+07	1.43E+08	2.36E+08	4.95E+08	1.99E+09
175	6.59E+07	9.80E+07	1.62E+08	3.39E+08	1.36E+09
200	4.71E+07	7.01E+07	1.16E+08	2.42E+08	9.73E+08
225	3.47E+07	5.17E+07	8.52E+07	1.79E+08	7.17E+08
250	2.63E+07	3.91E+07	6.44E+07	1.35E+08	5.43E+08
275	2.03E+07	3.02E+07	4.97E+07	1.04E+08	4.19E+08
300	1.59E+07	2.37E+07	3.91E+07	8.20E+07	3.29E+08

Table A2

Spacecraft Incident Solar Proton Fluences for 3 Solar Active Years

Values Do Not Include Design Margins

Energy	**Confidence Level**				
(>MeV)	80%	85%	90%	95%	99%
1	3.64E+11	4.20E+11	5.03E+11	6.57E+11	1.08E+12
3	1.29E+11	1.49E+11	1.80E+11	2.37E+11	3.96E+11
5	7.71E+10	9.09E+10	1.12E+11	1.52E+11	2.72E+11
7	5.55E+10	6.66E+10	8.39E+10	1.18E+11	2.24E+11
10	3.55E+10	4.50E+10	6.08E+10	9.47E+10	2.18E+11
15	2.06E+10	2.65E+10	3.63E+10	5.79E+10	1.39E+11
20	1.33E+10	1.73E+10	2.41E+10	3.95E+10	9.95E+10
25	9.28E+09	1.23E+10	1.76E+10	2.97E+10	7.97E+10
30	6.84E+09	9.25E+09	1.35E+10	2.38E+10	6.86E+10
35	5.26E+09	7.27E+09	1.09E+10	2.01E+10	6.26E+10
40	4.16E+09	5.88E+09	9.09E+09	1.74E+10	5.83E+10
45	3.30E+09	4.74E+09	7.47E+09	1.47E+10	5.19E+10
50	2.63E+09	3.81E+09	6.08E+09	1.21E+10	4.44E+10
55	2.11E+09	3.07E+09	4.92E+09	9.92E+09	3.69E+10
60	1.70E+09	2.48E+09	3.98E+09	8.05E+09	3.01E+10
70	1.13E+09	1.64E+09	2.64E+09	5.31E+09	1.98E+10
80	7.82E+08	1.14E+09	1.81E+09	3.64E+09	1.34E+10
90	5.63E+08	8.18E+08	1.31E+09	2.63E+09	9.72E+09
100	4.15E+08	6.05E+08	9.73E+08	1.97E+09	7.38E+09
125	2.50E+08	3.65E+08	5.87E+08	1.19E+09	4.45E+09
150	1.62E+08	2.36E+08	3.80E+08	7.69E+08	2.88E+09
175	1.11E+08	1.62E+08	2.60E+08	5.26E+08	1.97E+09
200	7.93E+07	1.16E+08	1.86E+08	3.76E+08	1.41E+09
225	5.84E+07	8.53E+07	1.37E+08	2.78E+08	1.04E+09
250	4.42E+07	6.45E+07	1.04E+08	2.10E+08	7.87E+08
275	3.41E+07	4.98E+07	8.01E+07	1.62E+08	6.07E+08
300	2.68E+07	3.91E+07	6.30E+07	1.27E+08	4.78E+08

Table A3
Spacecraft Incident Solar Proton Fluences for 4 Solar Active Years
Values Do Not Include Design Margins

Energy	Confidence Level				
(>MeV)	80%	85%	90%	95%	99%
1	4.80E+11	5.46E+11	6.41E+11	8.13E+11	1.27E+12
3	1.70E+11	1.94E+11	2.29E+11	2.93E+11	4.63E+11
5	1.02E+11	1.19E+11	1.43E+11	1.89E+11	3.19E+11
7	7.43E+10	8.77E+10	1.08E+11	1.47E+11	2.63E+11
10	4.88E+10	6.08E+10	8.02E+10	1.21E+11	2.61E+11
15	2.85E+10	3.60E+10	4.82E+10	7.44E+10	1.68E+11
20	1.85E+10	2.36E+10	3.22E+10	5.11E+10	1.21E+11
25	1.30E+10	1.69E+10	2.37E+10	3.88E+10	9.80E+10
30	9.65E+09	1.28E+10	1.84E+10	3.14E+10	8.52E+10
35	7.47E+09	1.02E+10	1.50E+10	2.67E+10	7.88E+10
40	5.95E+09	8.29E+09	1.26E+10	2.33E+10	7.43E+10
45	4.74E+09	6.71E+09	1.04E+10	1.98E+10	6.66E+10
50	3.79E+09	5.41E+09	8.46E+09	1.64E+10	5.72E+10
55	3.04E+09	4.36E+09	6.87E+09	1.35E+10	4.77E+10
60	2.45E+09	3.52E+09	5.55E+09	1.09E+10	3.89E+10
70	1.63E+09	2.34E+09	3.68E+09	7.22E+09	2.55E+10
80	1.13E+09	1.61E+09	2.53E+09	4.93E+09	1.73E+10
90	8.10E+08	1.16E+09	1.82E+09	3.57E+09	1.25E+10
100	5.98E+08	8.60E+08	1.36E+09	2.68E+09	9.54E+09
125	3.61E+08	5.19E+08	8.19E+08	1.61E+09	5.75E+09
150	2.33E+08	3.36E+08	5.30E+08	1.04E+09	3.72E+09
175	1.60E+08	2.30E+08	3.63E+08	7.15E+08	2.55E+09
200	1.14E+08	1.64E+08	2.60E+08	5.11E+08	1.82E+09
225	8.43E+07	1.21E+08	1.91E+08	3.77E+08	1.34E+09
250	6.37E+07	9.16E+07	1.45E+08	2.85E+08	1.02E+09
275	4.92E+07	7.07E+07	1.12E+08	2.20E+08	7.85E+08
300	3.87E+07	5.56E+07	8.79E+07	1.73E+08	6.17E+08

Table A4
Integral Solar Proton Fluence Levels Behind Solid Sphere Aluminum Shields
2 Active Solar Years – 95% Confidence Level
Values Do Not Include Design Margins

Degraded Energy	Shielded Solar Proton Fluences			
	50 mils Al (1.27 mm)	100 mils Al (2.54 mm)	200 mils Al (5.08 mm)	500 mils Al (12.7 mm)
> MeV	#/cm^2	#/cm^2	#/cm^2	#/cm^2
1.00E-01	3.89E+10	2.26E+10	1.38E+10	6.06E+09
1.26E-01	3.89E+10	2.26E+10	1.38E+10	6.06E+09
1.58E-01	3.89E+10	2.26E+10	1.38E+10	6.06E+09
2.00E-01	3.89E+10	2.26E+10	1.38E+10	6.06E+09
2.51E-01	3.89E+10	2.26E+10	1.38E+10	6.06E+09
3.16E-01	3.89E+10	2.26E+10	1.38E+10	6.06E+09
3.98E-01	3.89E+10	2.26E+10	1.37E+10	6.06E+09
5.01E-01	3.88E+10	2.26E+10	1.37E+10	6.06E+09
6.31E-01	3.88E+10	2.26E+10	1.37E+10	6.06E+09
7.94E-01	3.87E+10	2.25E+10	1.37E+10	6.05E+09
1.00E+00	3.86E+10	2.25E+10	1.37E+10	6.05E+09
1.26E+00	3.85E+10	2.25E+10	1.37E+10	6.05E+09
1.58E+00	3.83E+10	2.24E+10	1.37E+10	6.04E+09
2.00E+00	3.80E+10	2.23E+10	1.37E+10	6.04E+09
2.51E+00	3.76E+10	2.22E+10	1.36E+10	6.03E+09
3.16E+00	3.70E+10	2.20E+10	1.36E+10	6.01E+09
3.98E+00	3.62E+10	2.17E+10	1.35E+10	5.99E+09
5.01E+00	3.51E+10	2.13E+10	1.34E+10	5.95E+09
6.31E+00	3.35E+10	2.08E+10	1.33E+10	5.90E+09
7.94E+00	3.13E+10	2.01E+10	1.30E+10	5.82E+09
1.00E+01	2.86E+10	1.91E+10	1.27E+10	5.70E+09
1.26E+01	2.55E+10	1.79E+10	1.22E+10	5.53E+09
1.58E+01	2.20E+10	1.63E+10	1.16E+10	5.26E+09
2.00E+01	1.84E+10	1.45E+10	1.08E+10	4.92E+09
2.51E+01	1.51E+10	1.26E+10	9.62E+09	4.42E+09
3.16E+01	1.23E+10	1.06E+10	8.22E+09	3.84E+09
3.98E+01	9.44E+09	8.19E+09	6.40E+09	3.12E+09
5.01E+01	6.35E+09	5.63E+09	4.42E+09	2.38E+09
6.31E+01	3.65E+09	3.36E+09	2.76E+09	1.69E+09
7.94E+01	1.91E+09	1.84E+09	1.63E+09	1.12E+09
1.00E+02	9.88E+08	9.74E+08	9.26E+08	7.43E+08
1.26E+02	5.52E+08	5.47E+08	5.33E+08	4.55E+08
1.58E+02	2.87E+08	2.85E+08	2.81E+08	2.51E+08
2.00E+02	1.27E+08	1.26E+08	1.25E+08	1.16E+08
2.51E+02	3.52E+07	3.52E+07	3.52E+07	3.22E+07

Table A5
Integral Solar Proton Fluence Levels Behind Solid Sphere Aluminum Shields
3 Active Solar Years – 95% Confidence Level
Values Do Not Include Design Margins

Degraded Energy	Shielded Solar Proton Fluences			
	50 mils Al (1.27 mm)	100 mils Al (2.54 mm)	200 mils Al (5.08 mm)	500 mils Al (12.7 mm)
> MeV	#/cm^2	#/cm^2	#/cm^2	#/cm^2
1.00E-01	5.62E+10	3.31E+10	2.07E+10	9.40E+09
1.26E-01	5.62E+10	3.31E+10	2.07E+10	9.40E+09
1.58E-01	5.62E+10	3.31E+10	2.07E+10	9.40E+09
2.00E-01	5.62E+10	3.31E+10	2.07E+10	9.40E+09
2.51E-01	5.61E+10	3.31E+10	2.07E+10	9.40E+09
3.16E-01	5.61E+10	3.31E+10	2.07E+10	9.40E+09
3.98E-01	5.61E+10	3.31E+10	2.07E+10	9.40E+09
5.01E-01	5.60E+10	3.30E+10	2.06E+10	9.39E+09
6.31E-01	5.60E+10	3.30E+10	2.06E+10	9.39E+09
7.94E-01	5.59E+10	3.30E+10	2.06E+10	9.39E+09
1.00E+00	5.58E+10	3.30E+10	2.06E+10	9.39E+09
1.26E+00	5.56E+10	3.29E+10	2.06E+10	9.38E+09
1.58E+00	5.53E+10	3.28E+10	2.06E+10	9.37E+09
2.00E+00	5.49E+10	3.27E+10	2.06E+10	9.36E+09
2.51E+00	5.43E+10	3.25E+10	2.05E+10	9.35E+09
3.16E+00	5.35E+10	3.23E+10	2.04E+10	9.32E+09
3.98E+00	5.23E+10	3.19E+10	2.03E+10	9.29E+09
5.01E+00	5.07E+10	3.13E+10	2.02E+10	9.23E+09
6.31E+00	4.85E+10	3.06E+10	1.99E+10	9.15E+09
7.94E+00	4.54E+10	2.96E+10	1.96E+10	9.03E+09
1.00E+01	4.15E+10	2.81E+10	1.92E+10	8.85E+09
1.26E+01	3.72E+10	2.64E+10	1.86E+10	8.58E+09
1.58E+01	3.23E+10	2.42E+10	1.77E+10	8.17E+09
2.00E+01	2.73E+10	2.17E+10	1.66E+10	7.64E+09
2.51E+01	2.26E+10	1.90E+10	1.48E+10	6.86E+09
3.16E+01	1.87E+10	1.62E+10	1.27E+10	5.95E+09
3.98E+01	1.46E+10	1.27E+10	9.91E+09	4.83E+09
5.01E+01	9.83E+09	8.73E+09	6.86E+09	3.68E+09
6.31E+01	5.65E+09	5.20E+09	4.28E+09	2.61E+09
7.94E+01	2.96E+09	2.85E+09	2.52E+09	1.74E+09
1.00E+02	1.53E+09	1.51E+09	1.44E+09	1.16E+09
1.26E+02	8.59E+08	8.51E+08	8.29E+08	7.08E+08
1.58E+02	4.45E+08	4.43E+08	4.37E+08	3.89E+08
2.00E+02	1.98E+08	1.97E+08	1.95E+08	1.81E+08
2.51E+02	5.58E+07	5.58E+07	5.58E+07	5.11E+07

Table A6
Integral Solar Proton Fluence Levels Behind Solid Sphere Aluminum Shields
4 Active Solar Years – 95% Confidence Level
Values Do Not Include Design Margins

Degraded Energy	Shielded Solar Proton Fluences			
	50 mils Al (1.27 mm)	100 mils Al (2.54 mm)	200 mils Al (5.08 mm)	500 mils Al (12.7 mm)
> MeV	#/cm^2	#/cm^2	#/cm^2	#/cm^2
1.00E-01	7.22E+10	4.30E+10	2.73E+10	1.28E+10
1.26E-01	7.22E+10	4.30E+10	2.73E+10	1.28E+10
1.58E-01	7.22E+10	4.30E+10	2.73E+10	1.28E+10
2.00E-01	7.22E+10	4.30E+10	2.73E+10	1.28E+10
2.51E-01	7.21E+10	4.30E+10	2.73E+10	1.28E+10
3.16E-01	7.21E+10	4.29E+10	2.73E+10	1.28E+10
3.98E-01	7.21E+10	4.29E+10	2.73E+10	1.28E+10
5.01E-01	7.20E+10	4.29E+10	2.73E+10	1.28E+10
6.31E-01	7.19E+10	4.29E+10	2.73E+10	1.28E+10
7.94E-01	7.18E+10	4.29E+10	2.73E+10	1.28E+10
1.00E+00	7.17E+10	4.28E+10	2.73E+10	1.28E+10
1.26E+00	7.14E+10	4.27E+10	2.73E+10	1.27E+10
1.58E+00	7.11E+10	4.26E+10	2.72E+10	1.27E+10
2.00E+00	7.06E+10	4.25E+10	2.72E+10	1.27E+10
2.51E+00	6.98E+10	4.23E+10	2.71E+10	1.27E+10
3.16E+00	6.87E+10	4.19E+10	2.71E+10	1.27E+10
3.98E+00	6.73E+10	4.14E+10	2.69E+10	1.26E+10
5.01E+00	6.53E+10	4.07E+10	2.67E+10	1.25E+10
6.31E+00	6.24E+10	3.98E+10	2.64E+10	1.24E+10
7.94E+00	5.86E+10	3.85E+10	2.60E+10	1.23E+10
1.00E+01	5.36E+10	3.67E+10	2.55E+10	1.20E+10
1.26E+01	4.82E+10	3.46E+10	2.47E+10	1.16E+10
1.58E+01	4.20E+10	3.18E+10	2.36E+10	1.11E+10
2.00E+01	3.58E+10	2.86E+10	2.22E+10	1.03E+10
2.51E+01	2.99E+10	2.53E+10	1.99E+10	9.30E+09
3.16E+01	2.48E+10	2.17E+10	1.71E+10	8.08E+09
3.98E+01	1.97E+10	1.71E+10	1.35E+10	6.56E+09
5.01E+01	1.34E+10	1.19E+10	9.30E+09	4.98E+09
6.31E+01	7.68E+09	7.07E+09	5.80E+09	3.54E+09
7.94E+01	4.00E+09	3.87E+09	3.42E+09	2.37E+09
1.00E+02	2.08E+09	2.05E+09	1.95E+09	1.56E+09
1.26E+02	1.16E+09	1.15E+09	1.12E+09	9.56E+08
1.58E+02	6.03E+08	6.00E+08	5.92E+08	5.28E+08
2.00E+02	2.67E+08	2.66E+08	2.64E+08	2.44E+08
2.51E+02	7.50E+07	7.50E+07	7.50E+07	6.86E+07

Table A7
Total Ionizing Dose at the Center of Aluminum Spheres Due to Solar Proton Events
95% Confidence Level
Values Do Not Include Design Margins

Aluminum Shield Thickness			2 Solar Active Years	3 Solar Active Years	4 Solar Active Years
g/cm^2	mm	mils	krads-si	krads-si	krads-si
0.03	0.11	4.37	1.51E+02	2.02E+02	2.48E+02
0.04	0.15	5.83	1.15E+02	1.54E+02	1.89E+02
0.05	0.19	7.29	8.96E+01	1.19E+02	1.46E+02
0.06	0.22	8.75	7.74E+01	1.03E+02	1.26E+02
0.08	0.30	11.67	6.16E+01	8.16E+01	9.90E+01
0.10	0.37	14.58	5.03E+01	6.64E+01	7.99E+01
0.15	0.56	21.87	4.05E+01	5.60E+01	6.98E+01
0.20	0.74	29.16	3.35E+01	4.75E+01	6.03E+01
0.30	1.11	43.74	2.17E+01	3.08E+01	3.92E+01
0.40	1.48	58.31	1.59E+01	2.26E+01	2.87E+01
0.50	1.85	72.91	1.18E+01	1.68E+01	2.14E+01
0.60	2.22	87.48	9.65E+00	1.37E+01	1.74E+01
0.80	2.96	116.65	6.81E+00	9.77E+00	1.25E+01
1.00	3.70	145.83	5.23E+00	7.57E+00	9.74E+00
1.25	4.63	182.28	4.02E+00	5.87E+00	7.63E+00
1.50	5.56	218.74	3.48E+00	5.07E+00	6.61E+00
1.75	6.48	255.16	3.03E+00	4.51E+00	5.92E+00
2.00	7.41	291.61	2.72E+00	4.16E+00	5.50E+00
2.50	9.26	364.53	2.21E+00	3.41E+00	4.56E+00
3.00	11.11	437.40	1.84E+00	2.83E+00	3.82E+00
3.50	12.96	510.24	1.48E+00	2.29E+00	3.13E+00
4.00	14.81	583.07	1.20E+00	1.88E+00	2.53E+00
4.50	16.67	656.30	9.57E-01	1.49E+00	2.02E+00
5.00	18.52	729.13	7.73E-01	1.20E+00	1.63E+00
5.50	20.37	801.97	6.62E-01	1.02E+00	1.40E+00
6.00	22.22	874.80	5.43E-01	8.40E-01	1.14E+00
6.50	24.07	947.64	4.58E-01	7.10E-01	9.60E-01
7.00	25.93	1020.87	3.92E-01	6.07E-01	8.20E-01
7.50	27.78	1093.70	3.38E-01	5.22E-01	7.07E-01
8.00	29.63	1166.54	2.98E-01	4.60E-01	6.23E-01
8.50	31.48	1239.37	2.61E-01	4.02E-01	5.45E-01
9.00	33.33	1312.20	2.30E-01	3.56E-01	4.83E-01
9.50	35.19	1385.43	2.01E-01	3.10E-01	4.22E-01
10.00	37.04	1458.27	1.69E-01	2.62E-01	3.58E-01
12.50	46.30	1822.83	1.23E-01	1.90E-01	2.59E-01
15.00	55.56	2187.40	9.00E-02	1.40E-01	1.90E-01
20.00	74.07	2916.14	5.36E-02	8.34E-02	1.12E-01
25.00	92.59	3645.28	3.40E-02	5.27E-02	7.16E-02
30.00	111.10	4374.02	2.30E-02	3.57E-02	4.86E-02

Table A8
Integral LET for Interplanetary Galactic Cosmic Rays (Z=1-92)
100 mils Aluminum Shielding
Values Do Not Include Design Margins

LET	LET Fluence	LET	LET Fluence
MeV*cm/mg	#/sqcm/day	MeV*sqcm/mg	#/sqcm/day
	Solar Minimum		Solar Maximum
0.10	2.23E+03	0.10	8.73E+02
0.20	9.84E+02	0.20	3.59E+02
0.40	4.33E+02	0.40	1.52E+02
0.60	2.90E+02	0.60	1.10E+02
0.80	2.23E+02	0.80	8.84E+01
1.00	1.79E+02	1.00	7.22E+01
2.01	3.39E+01	2.01	5.88E+00
3.02	1.43E+01	3.02	2.03E+00
3.99	7.76E+00	3.99	1.02E+00
5.03	4.59E+00	5.03	5.81E-01
5.99	3.07E+00	5.99	3.80E-01
8.00	1.55E+00	8.00	1.90E-01
10.09	9.00E-01	10.09	1.10E-01
11.07	7.17E-01	11.07	8.75E-02
12.01	5.76E-01	12.01	7.04E-02
13.02	4.67E-01	13.02	5.71E-02
13.96	3.85E-01	13.96	4.72E-02
14.97	3.16E-01	14.97	3.88E-02
16.05	2.61E-01	16.05	3.20E-02
17.00	2.20E-01	17.00	2.71E-02
18.02	1.85E-01	18.02	2.27E-02
19.09	1.54E-01	19.09	1.89E-02
20.00	1.30E-01	20.00	1.60E-02
24.93	4.45E-02	24.93	5.50E-03
30.01	6.27E-04	30.01	8.18E-05
34.90	6.86E-05	34.90	1.06E-05
40.11	4.18E-05	40.11	6.50E-06
45.04	2.83E-05	45.04	4.42E-06
49.99	2.00E-05	49.99	3.13E-06
50.58	1.92E-05	50.58	3.00E-06
55.49	1.34E-05	55.49	2.11E-06
60.19	9.38E-06	60.19	1.49E-06
65.28	6.32E-06	65.28	1.01E-06
69.98	4.40E-06	69.98	7.01E-07
75.02	2.83E-06	75.02	4.52E-07
80.43	1.65E-06	80.43	2.63E-07

Table A8 (Continued)
Integral LET for Interplanetary Galactic Cosmic Rays (Z=1-92)
100 mils Aluminum Shielding
Values Do Not Include Design Margins

LET	LET Fluence	LET	LET Fluence
MeV*cm/mg	#/sqcm/day	MeV*sqcm/mg	#/sqcm/day
	Solar Minimum		Solar Maximum
85.23	7.71E-07	85.23	1.23E-07
90.32	1.94E-07	90.32	3.10E-08
95.71	2.88E-08	95.71	4.60E-09
100.25	1.19E-08	100.25	1.89E-09
101.42	5.27E-09	101.42	8.41E-10
102.61	2.54E-09	102.61	4.05E-10

Table A9

Integral LET for the October 1989 Solar Particle Event (Z=1-92)

100 mils Aluminum Shielding

Values Do Not Include Design Margins

LET	LET Fluence	LET Fluence	LET Fluence
MeV*cm^2/mg	#/cm^2/s	#/cm^2/s	#/cm^2/s
	Average Over Peak	Average Over Worst Day	Average Over Worst Week
0.10	5.16E+02	1.37E+02	2.27E+01
0.20	1.75E+02	4.63E+01	7.53E+00
0.30	7.90E+01	2.09E+01	3.45E+00
0.40	4.36E+01	1.15E+01	1.95E+00
0.50	2.75E+01	7.30E+00	1.26E+00
0.60	1.86E+01	4.94E+00	8.78E-01
0.70	1.35E+01	3.58E+00	6.52E-01
0.81	9.85E+00	2.62E+00	4.91E-01
0.90	7.55E+00	2.02E+00	3.87E-01
1.00	5.88E+00	1.57E+00	3.10E-01
2.01	7.49E-01	2.06E-01	5.99E-02
3.02	4.11E-01	1.13E-01	3.33E-02
3.99	2.64E-01	7.29E-02	2.14E-02
5.03	1.74E-01	4.80E-02	1.42E-02
6.06	1.21E-01	3.36E-02	9.92E-03
7.04	8.68E-02	2.40E-02	7.11E-03
8.00	6.39E-02	1.77E-02	5.26E-03
8.99	5.04E-02	1.40E-02	4.13E-03
10.09	3.85E-02	1.07E-02	3.15E-03
20.00	5.75E-03	1.60E-03	4.63E-04
25.22	2.14E-03	5.95E-04	1.72E-04
30.01	1.83E-05	5.10E-06	1.55E-06
35.30	7.23E-07	2.01E-07	7.14E-08
40.11	3.26E-07	9.08E-08	3.43E-08
45.04	1.95E-07	5.44E-08	2.12E-08
49.99	1.36E-07	3.78E-08	1.48E-08
55.49	8.43E-08	2.35E-08	9.31E-09
60.19	4.92E-08	1.37E-08	5.58E-09
65.28	3.28E-08	9.12E-09	3.75E-09
69.98	2.49E-08	6.92E-09	2.84E-09
75.02	1.80E-08	5.00E-09	2.04E-09
80.43	1.20E-08	3.34E-09	1.36E-09
85.23	6.69E-09	1.86E-09	7.56E-10
90.32	2.03E-09	5.64E-10	2.29E-10
94.61	1.33E-10	3.71E-11	1.51E-11
100.25	5.01E-11	1.39E-11	5.66E-12
101.42	2.22E-11	6.19E-12	2.51E-12
102.61	1.07E-11	2.99E-12	1.21E-12

Table A10

Differential Fluxes from Solar Proton Events

100 mils Aluminum Shielding, CREME96

Note: Spectra were cut off at E =1 MeV and E=1000 MeV

Values Do Not Include Design Margins

Energy	**Proton Flux**	**Proton Flux**	**Proton Flux**
MeV	#/cm^2/s	#/cm^2/s	#/cm^2/s
	Average Over Peak	Average Over Worst Day	Average Over Worst Week
1.00	1.75E+03	4.62E+02	8.85E+01
2.00	2.68E+03	7.09E+02	1.36E+02
3.02	3.47E+03	9.17E+02	1.76E+02
4.04	4.11E+03	1.09E+03	2.09E+02
5.04	4.62E+03	1.22E+03	2.36E+02
6.03	5.03E+03	1.33E+03	2.58E+02
7.02	5.33E+03	1.41E+03	2.75E+02
8.06	5.56E+03	1.47E+03	2.88E+02
9.00	5.69E+03	1.51E+03	2.96E+02
10.05	5.76E+03	1.53E+03	3.01E+02
14.99	5.41E+03	1.44E+03	2.92E+02
20.03	4.50E+03	1.21E+03	2.52E+02
24.98	3.57E+03	9.65E+02	2.07E+02
30.31	2.73E+03	7.40E+02	1.64E+02
35.27	2.11E+03	5.75E+02	1.31E+02
40.49	1.61E+03	4.42E+02	1.04E+02
50.50	9.91E+02	2.73E+02	6.79E+01
60.43	6.33E+02	1.75E+02	4.58E+01
70.33	4.20E+02	1.17E+02	3.20E+01
79.63	2.94E+02	8.18E+01	2.33E+01
90.17	2.03E+02	5.65E+01	1.68E+01
100.69	1.44E+02	4.01E+01	1.24E+01
150.25	3.84E+01	1.06E+01	3.80E+00
200.77	1.39E+01	3.79E+00	1.50E+00
299.59	3.32E+00	8.62E-01	3.88E-01
400.31	1.16E+00	2.85E-01	1.39E-01
499.23	4.97E-01	1.16E-01	5.96E-02
605.64	2.07E-01	4.64E-02	2.54E-02
704.94	1.10E-01	2.48E-02	1.44E-02
798.17	6.61E-02	1.48E-02	9.03E-03
903.74	3.95E-02	8.88E-03	5.66E-03
995.41	2.65E-02	5.96E-03	3.94E-03